Journal of Medicinal Chemistry

pubs.acs.org/jmc

Article

One-Pot Procedure for the Synthesis of Asymmetric Substituted Ureido Benzene Sulfonamides as Effective Inhibitors of Carbonic Anhydrase Enzymes

Gioele Vannozzi, Daniela Vullo, Andrea Angeli, Marta Ferraroni, Jacob Combs, Carrie Lomelino, Jacob Andring, Robert Mckenna, Gianluca Bartolucci, Marco Pallecchi, Laura Lucarini, Silvia Sgambellone, Emanuela Masini, Fabrizio Carta,* and Claudiu T. Supuran*

Cite This: *J. Med. Chem.* 2022, 65, 824−837

Read Online

ACCESS | Metrics & More | Article Recommendations | Supporting Information

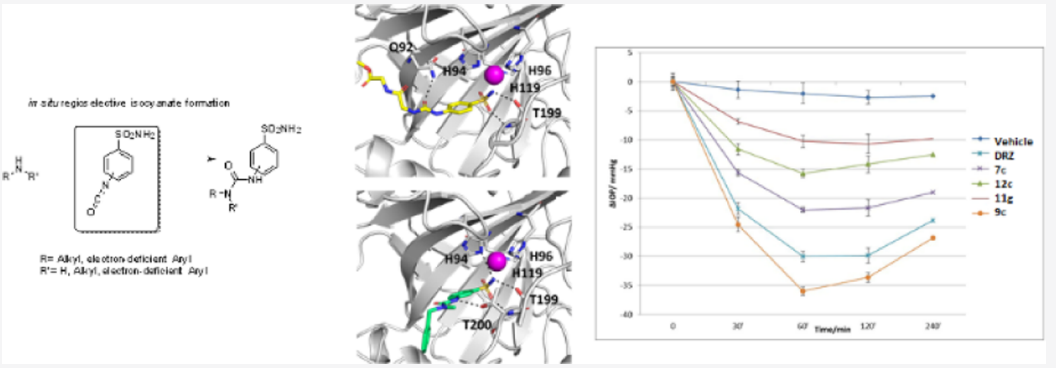

ABSTRACT: We report a one-pot procedure for the synthesis of asymmetrical ureido-containing benzenesulfonamides based on in situ generation of the corresponding isocyanatobenezenesulfonamide species, which were trapped with the appropriate amines. A library of new compounds was generated and evaluated in vitro for their inhibition properties against a representative panel of the human (h) metalloenzymes carbonic anhydrases (EC 4.2.1.1), and the best performing compounds on the isozyme II (i.e., **7c**, **9c**, **11g**, and **12c**) were screened for their ability to reduce the intraocular pressure in glaucomatous rabbits. In addition, the binding modes of **7c**, **11f**, and **11g** were assessed by means of X-ray crystallography.

INTRODUCTION

The ureido moiety is widely represented in medicinal chemistry as being part of a multitude of compounds of natural or synthetic sources for which biomedical and/or technological applications are reported.[1−8] The reasons behind such a vast diffusion of this group are generally ascribed to: (i) its capability to efficiently establish hydrogen bond interactions with biological targets of interest (i.e., proteins and/or nucleic acids); (ii) it allows the *N*-substituents to adopt suitable conformations as needed; and (iii) it possesses physicochemical features that endow the ligands with suitable drug-ability performance.[1,6,7] More importantly, the above features are all adequately and easily tunable by means of appropriate chemical manipulation/substitution of the *N*-groups inserted.[1,9,10] Many scientific studies dealing with the ureido group within the context of modern medicinal chemistry, biology, and technology are periodically reported. Among them are the research studies of some of us on the identification of ureido-containing small molecules as effective inhibitors of the carbonic anhydrase (CA, EC 4.2.1.1) enzymes and potential use for biomedical purposes.[11−17] On the course of our investigations, we encountered synthetic limitations to access asymmetrical ureido-substituted benzenesulfonamides via in situ generation of highly instable isocyanates from primary amines of the alkyl type or anilines on electron-deficient aryl substrates (Figure 1A).

The high reliability, practicality, cost-effectiveness, and environmental-friendly features of such an approach, compared to alternative synthetic methods,[18] triggered us to set a one-pot procedure based on the efficient in situ conversion of the aniline moiety of commercially available arylsulfonamides into isocyanates (Figure 1B). This approach is also useful to make use of secondary amines as nucleophilic agents to obtain one-pot *N,N*-substituted ureido derivatives of the type reported in Figure 1B. To the best of our knowledge, the current procedures mainly

Received: November 5, 2021
Published: December 27, 2021

Downloaded via UNIV DEGLI STUDI DI FIRENZE on January 24, 2025 at 11:10:17 (UTC).
See https://pubs.acs.org/sharingguidelines for options on how to legitimately share published articles.

ACS Publications

© 2021 American Chemical Society

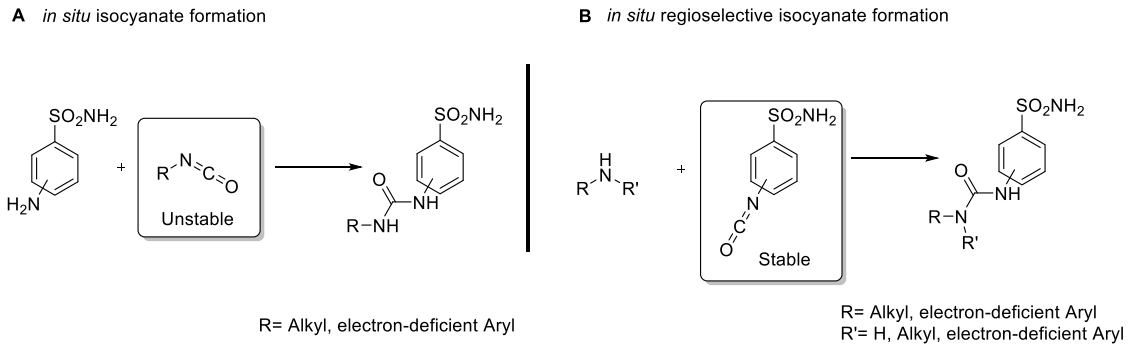

Figure 1. General scheme for the synthesis of asymmetrical ureido compounds.

Scheme 1. Expected Reaction Pathways for the Treatment of Sulfanilamide 1a with Phosgene or Triphosgene

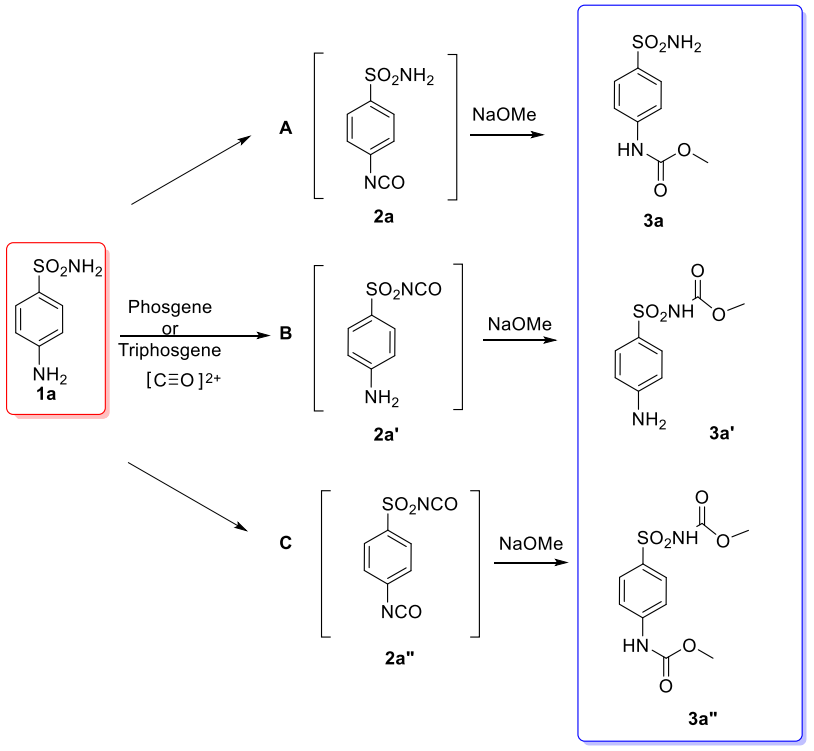

rely on the isolation of the arylsulfonamide isocyanate species, which is trapped afterward with the desired amine to afford the ureido derivative.[19−22]

RESULTS AND DISCUSSION

Design and Synthesis of Compounds. We established a synthetic strategy aimed at obtaining asymmetrical ureido derivatives bearing the carbonic anhydrase inhibitor (CAI) warhead of the arylsulfonamide type by assembling the commercially available sulfanilamide **1a** and metanilamide **1b** with either secondary or primary alkylamines upon in situ generation of the appropriate aryl isocyanates. Such a synthetic approach proved to be not of immediate applicability for our purposes as (i) two functional groups in **1a** and **1b** (i.e., the primary sulfonamide and the aniline) were both able to competitively generate isocyanates; (ii) since we aimed at setting a convenient synthetic strategy of immediate use to address the formation of the key moiety isocyanate, the materials were required not to be subjected to unnecessary manipulations such as the introduction of protecting groups; and (iii) to the best of our knowledge, no synthetic protocol of this type was reported in the literature.

First, we turned our attention to the formation of the key intermediate isocyanato benezenesulfonamide **2a** avoiding the competitive generation of the benzenesulfonylisocyanate **2a'** and the isocyanato benzenesulfonylisocyanate **2a″** when the starting material **1a** was treated either with phosgene or triphosgene (Scheme 1A−C).

We performed our investigations on sulfanilamide **1a** as the substrate rather than metanilamide **1b** since its aniline moiety is far less nucleophilic toward the formal acylium dication species $[C{\equiv}O]^{2+}$ and that makes the reaction challenging to direct onto the pathway in Scheme 1A. Conversely, the electron-withdrawing effect of sulfonamide on the aniline moiety is highly reduced within the regioisomer **1b**. This substrate is not expected to undergo a competitive pathway when subjected to a synthetic protocol established for **1a**. The reaction quenched with 2.1 equiv of freshly prepared sodium methoxide was intended as an effective way to trap the in situ isocyanate species formed by means of their corresponding ureido derivatives **3a-**

https://doi.org/10.1021/acs.jmedchem.1c01906
J. Med. Chem. 2022, 65, 824−837

Scheme 2. Synthesis of 4-Ureido Benzenesulfonamide Derivatives 7−9

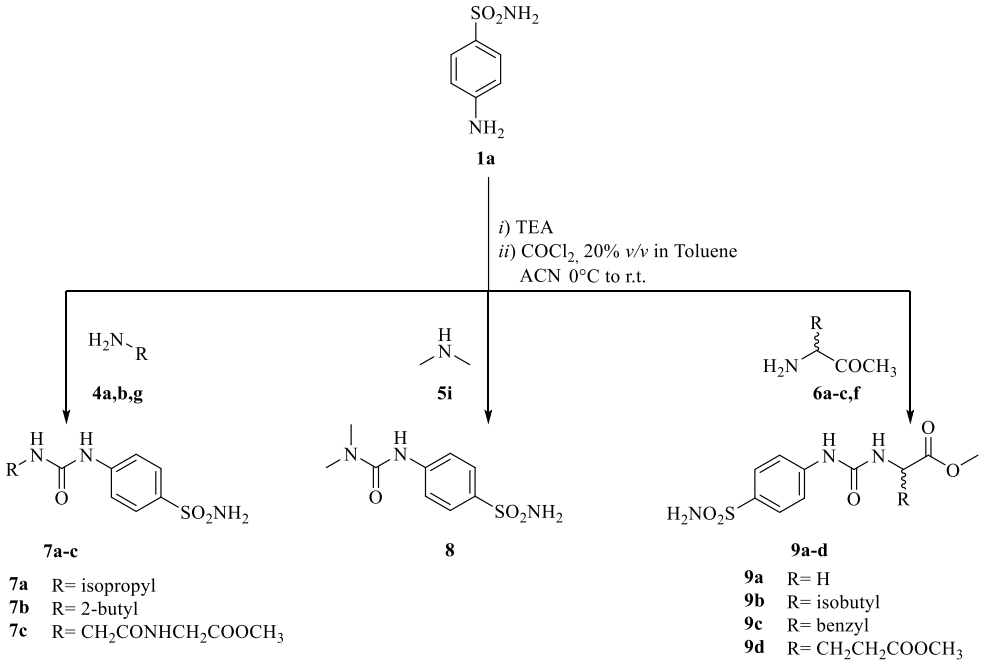

Scheme 3. Synthesis of 3-Ureido Benzenesulfonamide Derivatives 10−12

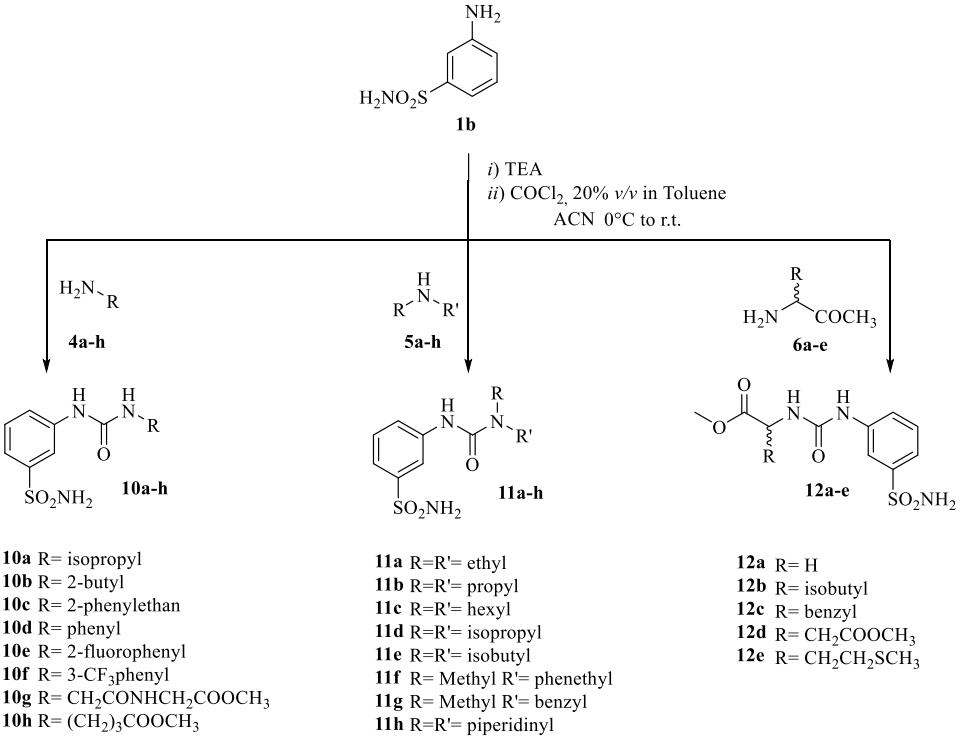

3a″easily identifiable by ^{1}H nuclear magnetic resonance (NMR) spectroscopy and comparable structural data in the literature.

Various reaction conditions were explored, and their outcomes are summarized in Table S1 in the Supporting Information. The best reaction conditions were treatment at 0 °C under a nitrogen atmosphere of a 2.0 M acetonitrile (ACN) solution of sulfanilamide **1a** and triethylamine (TEA, 5.0 equiv) with a commercially available 20% v/v solution of phosgene in toluene (1.5 equiv). The reaction mixture was stirred for 5 min and then quenched by dropwise addition of an appropriate nucleophile. In agreement with our previous studies, also in this study, the formation of the desired ureido moiety result was particularly favored when ACN was used as the solvent as it separates out of the solution as a precipitate.[11,12] Such a procedure was successfully applied to the synthesis of both 4- and 3-ureidobenzenesulfonamides with comparable yields among the two series (Schemes 2 and 3).

All the final compounds reported here were purified by silica gel column chromatography using appropriate eluting mixtures followed by trituration or recrystallization as needed. In

https://doi.org/10.1021/acs.jmedchem.1c01906
J. Med. Chem. 2022, 65, 824−837

addition, they were fully characterized by means of ^{1}H NMR, ^{13}C NMR, ^{19}F NMR, high-resolution mass spectrometry (HRMS), and elemental analyses. High-performance liquid chromatography (HPLC) traces are provided in the Supporting Information and they show a purity grade ≥95%.

In Vitro CA Inhibition. The inhibition profiles for the final compounds **7a−c**, **8**, **9a−d**, **10a−h**, **11a−h**, and **12a−e** and the reference drugs of the sulfonamide type acetazolamide (**AAZ**) and **SLC-0111** against the physiologically relevant hCAs I, II, IX, and XII are reported in Table 1. All data were determined by means of the stopped-flow CO_2 hydrase assay.[23] Table 1 includes the selectivity indexes (SIs) referred to the main isoform involved in intraocular pressure building (i.e., hCA II) over the off-target hCA IX.[15−17]

Table 1. Inhibition Data of 7a−c, 8, 9a−d, 10a−h, 11a−h, 12a−e, and the Standard Sulfonamide Inhibitor Acetazolamide (AAZ) and SLC-0111 against the hCAs I, II, IX, and XII by the Stopped-Flow CO_2 Hydrase Assay[23]

	K_I (nM)[a]				
compound	hCA I	hCA II	hCA IX	hCA XII	SIs (K_IhCA IX/K_IhCA II)
7a	438.2	9.2	640.5	592.7	69.6
7b	668.5	34.9	506.7	636.9	14.5
7c	7571	45.3	1571	426.4	34.7
8	482.7	8.1	1396	705.5	172.3
9a	802.3	23.9	1916	773.0	80.2
9b	225.8	1.5	937.5	586.0	625
9c	62.3	3.6	125.5	42.6	34.9
9d	62.0	2.8	596.0	725.6	212.9
10a	61.7	62.6	2167	612.5	34.6
10b	69.9	21.7	2122	600.0	97.8
10c	296.3	1.3	1329	486.8	1022
10d	449.4	0.89	1801	355.8	2023.6
10e	737.4	221.7	1479	511.6	6.7
10f	2061	41.5	1600	489.6	38.6
10g	7187	243.2	690.5	344.2	2.8
10h	8276	227.6	745.7	493.7	3.3
11a	2884	132.7	1727	374.7	13.0
11b	527.9	17.4	2195	532.3	126.1
11c	4955	3.2	2112	649.6	660
11d	1625	2752	2092	813.0	0.76
11e	1417	1636	1792	489.5	1.1
11f	921.6	1.6	1183	388.5	739.4
11g	73.6	9.3	1441	605.6	154.9
11h	177.6	92.2	540.5	277.9	5.9
12a	6074	446.2	825.0	465.8	1.8
12b	5284	714.6	839.2	589.4	1.2
12c	808.8	172.8	942.5	275.2	5.5
12d	8381	498.1	859.7	492.8	1.7
12e	1732	633.7	1383	426.0	2.2
AAZ	250.0	12.1	25.8	5.8	2.1
SLC-0111[12]	5080	960	45.1	4.5	0.04

[a]Mean from three different assays using the stopped-flow technique (errors were in the range of ±5 to 10% of the reported values).

The following structure−activity relationships (SARs) may be drawn from the inhibition data reported in Table 1:

(i) According to the data in Table 1, the whole compounds obtained were not particularly effective in inhibiting the hCA I isoform. Among the sulfanilamide series **7a−c** and **8**, the introduction of linear alkyl moieties at the distal ureido nitrogen such as the glycylglycine methyl ester (Gly-Gly-OMe) in **7c** was detrimental for the inhibition potency (K_I of 7571 nM). The remaining derivatives **7a**,**b** and **8** that contained bulky alkyl moieties instead were all more potent hCA I inhibitors (K_I values of 438.2, 668.5, and 482.7 nM, respectively) although far less active compared to the standard **AAZ** (K_I 250.0 nM). A similar kinetic trend was observed within the **9a−d** series with the glycine methyl ester (Gly-OMe) derivative **9a**, the weakest inhibitor (K_I of 802.3 nM). Substitution of the glycine tail in **9a** with branched amino acids such as (±)-leucine **9b**, (±)-phenylalanine **9c**, and (±)-glutamic acid methyl ester **9d** resulted in an increase of the ligand enzyme affinity up to 12.9-fold. Interestingly, both (±)-phenylalanine **9c** and the (±)-glutamic acid derivative **9d** were equally potent inhibitors (K_I values of 62.3 and 62.0 nM, respectively). It is worth noting that the Gly-OMe derivative **9a** resulted in a 9.4-fold more potent hCA I inhibitor compared to its longer Gly-Gly-OMe counterpart **7c** (K_I values of 802.3 and 7571 nM, respectively). A marked regioisomeric effect was observed for the metanilamide derivatives **10a** and **10b** compared to their sulfanilamide analogues **7a** and **7b**, the former being 7.1- and 9.6-fold more potent than the latter (K_I values of 61.7 and 69.9 nM for **10a** and **10b** and 438.2 and 668.5 nM for **7a** and **7b**). The same effect was not observed for the regioisomeric couple **10g** and **7c** bearing the Gly-Gly-OMe tail as they showed close-matching K_I values (i.e., 7187 and 7571 nM, respectively). A weak increase of the inhibition potency (i.e., 1.2-fold) was obtained when the Gly-Gly-OMe moiety in **10g** was shortened up to (±)-Gly-OMe as in **12a**. Substitution of the glycine amino acid in **12a** with (±)-leucine **12b** or (±)-phenylalanine **12c** instead resulted in a progressive increase of the inhibition potency against the hCA I isoform. Finally, the (±)-aspartate methyl ester **12d** and the (±)-methionine derivative **12e** showed K_I values of 8381 and 1732 nM, respectively. A rather difficult kinetic profile was observed when the distal ureido nitrogen was fully substituted as in compounds **11a−h**. In particular, the extension of the linear alkyl chains in **11a** up to *n*-propyl, as in **11b**, increased the inhibition potency up to 5.5-fold. A further increase in the chain length affected the hCA I inhibition potency as reported for compound **11c** (K_I value of 4955 nM). In analogy to **11c**, the introduction of symmetric and bulky alkyl chains also resulted in the reduction of the inhibition potency (see Table 1 for compounds **11d** and **11e**). Desymmetrization of the distal ureidic nitrogen as in compounds **11f** and **11g** gave interesting results only for the latter (i.e., bearing *N*-methyl and *N*-benzyl moieties). It is worth noting that the additional methylene in **11f** that afforded **11g** was fully responsible for a 12.5-fold increase of the hCA I inhibition potency (see Table 1).

(ii) As for the cytosolic and most abundantly expressed hCA II isoform, overall the compounds reported here resulted in far more efficient inhibitors and with definite SAR compared to the hCA I previously discussed (see Table 1). Among the sulfanilamide series, the bulky isopropyl derivative **10a** resulted in 1.3-fold more potent inhibition compared to the reference **AAZ** (K_I values of 9.2 and 12.1 nM, respectively). In analogy to hCA I, the introduction

https://doi.org/10.1021/acs.jmedchem.1c01906
J. Med. Chem. 2022, 65, 824−837

of linear substitution as in **7b** and **7c** also was detrimental for the inhibition potency for the isoform II (see Table 1). Again, the reduction of the Gly-Gly-OMe tail in **7c** with the -Gly-OMe moiety instead as in **9a** resulted in a 1.9-fold reduction of the K_I value (i.e., 45.3 and 23.9 nM, respectively). Interestingly, the inhibition potency increased when Gly-OMe in **9a** was substituted with (±)-leucine **9b**, (±)-phenylalanine **9c**, and (±)-aspartate methyl ester **9d.** As reported in Table 1, the experimentally obtained K_I values were 1.5, 3.6, and 2.8 nM, respectively, thus far lower when compared to the reference **AAZ** (i.e., K_I value of 12.1 nM). A slight increase in the inhibition value was obtained for compound **8** (K_I value of 8.1 nM), which was still more potent than the reference **AAZ**. A more defined kinetic profile was obtained for the metanilamide compound series. As reported in Table 1, a drastic reduction of the hCA II K_I values was obtained when the bulky isopropyl tail in **10a** (K_I value of 62.6 nM) was replaced with linear alkyl/alkylaryl moieties such as in **10b** and **10c** (K_I values of 21.7 and 1.3 nM, respectively). Interestingly, the simple phenyl derivative **10d** showed a remarkable subnanomolar K_I value of 0.89 nM, which drastically increased when a fluoro atom was introduced at position 2 of the aryl ring as in **10e** (K_I value of 221.7 nM). The regioisomer of **10e** (i.e., compound **10f**) bearing fluorine at position 3 resulted in 5.3-fold more potent inhibition (K_I value of 41.5 nM). The remaining compounds within this series (i.e., **10g** and **10h**) resulted in far more ineffective hCA II inhibitors (K_I values of 243.2 and 227.6 nM, respectively). Switching Gly-Gly-OMe in **10g** to the shorter Gly-OMe in **12a** enabled enhancement of the hCA II inhibition value up to 1.8-fold (K_I values of 243.2 and 446.2 nM, respectively). Changing the amino acid tail as in compounds **12b−e** did not significantly improve the inhibition potency and among them the (±)-phenylalanine derivative **12c** was the most potent with a K_I value of 172.8 nM. Interesting data were obtained for the distal *N,N*-disubstituted derivatives **11a−h**. Progressive reduction of the K_I values was observed when the linear alkyl chains were elongated up to the *n*-hexyl moiety as in **11a−c** (K_I values of 132.7, 17.4, and 3.2 nM for **11a**, **11b**, and **11c**, respectively). Conversely, the introduction of bulky substituents affected the potency as in **11d**, **11e**, and **11h** (K_I values of 2752, 1636, and 92.2 nM, respectively). The potency was restored when the distal ureido nitrogen was unsymmetrically substituted as in compounds **11f** and **11g**, which showed K_I values of 1.6 and 9.3 nM, respectively. It is worth noting that the insertion of a single carbon unit spacer in **11f** to afford the benzyl derivative **11g** deeply affected the kinetic value for the hCA II of 5.8-fold.

(iii) Overall, the compounds obtained showed weak inhibition potency for the tumor-associated hCA IX with K_I values spanning between 125.5 and 2167 nM, thus far less active compared to the reference **AAZ** (K_I value of 25.8 nM). Among the sulfanilamide series **7a−c**, isopropyl **7a** and 2-butan **7b** derivatives showed comparable inhibition potencies (K_I values of 640.5 and 506.7 nM, respectively), whereas the introduction of the longer Gly-Gly-OMe moiety as in **7c** significantly enhanced the K_I value up to 1571 nM (see Table 1). The insertion of the Gly-OMe tail as in **9a** resulted in a 1.2-fold decrease of the inhibition potency. Changing the amino acid moiety in **9a** with (±)-leucine **9b** (K_I value of 937.5 nM) and (±)-phenylalanine **9c** (K_I value of 125.5 nM) instead resulted in a progressive increase of the inhibition potency with the latter being the most potent hCA IX inhibitor among the sulfanilamide series screened. As reported in Table 1, the introduction of the (±)-aspartate methyl ester, as in compound **9d**, enabled significant enhancement of the hCA IX inhibition value (i.e., K_I value of 596.0 nM). Finally, disubstitution of the distal ureido nitrogen with the methyl moieties, as for compound **8**, also resulted in a micromolar potent inhibitor (see Table 1). As for the metanilamide series, a rather difficult SAR can be obtained from their kinetic profile reported in Table 1, which was almost flat. The most potent inhibitor among the metanilamide series was the disubstituted *N,N*-piperidine **11h** with a K_I value of 540.0 nM (see Table 1).

(iv) Interesting kinetic results were observed for the second tumor-associated isoform (i.e., hCA XII). Compounds **7a−c** showed an opposite inhibition profile trend against hCA XII compared to the primary tumor-related hCA IX, the 2-butan derivative **7b** being slightly less potent than the bulky isopropyl derivative **7a** (K_I values of 636.9 and 592.7 nM, respectively). Conversely, the insertion of the linear Gly-Gly-OMe moiety, as in **7c**, was beneficial for the inhibition potency as it resulted in up to 1.5-fold more active inhibition compared to the bulky **7b** (K_I values of 426.4 and 636.9 nM, respectively). In analogy to the hCA IX kinetic profile, it was reported that length reduction of the alkyl linear tail in **7c** to afford the Gly-OMe-substituted **9a** enhanced the K_I value to 1.8-fold for the hCA XII isoform (K_I values of 426.4 and 773.0 nM, respectively). The introduction of various amino acid moieties as tails to afford compounds **9b−d** also resulted in a kinetic trend for hCA XII, which was almost superimposable to the primarily tumor-associated isoform IX although with a different intensity. As reported in Table 1, the substitution of the Gly-OMe tail in **9a** with (±)-lysine or (±)-phenylalanine, as in **9b** and **9c**, respectively, resulted in a great enhancement of the inhibition potency with K_I values of 733.0, 586.0, and 42.6 nM, respectively. Again, the (±)-aspartate methyl ester derivative **9d** was detrimental for the inhibition potency (K_I value of 725.6 nM). As previously discussed for hCA IX, the metanilamide series also did not show a particularly interesting kinetic profile for the hCA XII isoform and the profile was almost flat. Data in Table 1 showed that the *N,N*-disubstituted piperidine **11h** and the (±)-phenylalanine methyl ester **12c** derivative were the most potent hCA XII inhibitors among the series with K_I values of 277.9 and 275.2 nM, respectively.

Overall, the in vitro kinetic profiles of compounds **7a−c**, **8**, **9a−d**, **10a−h**, **11a−h**, and **12a−e** on the hCAs I, II, IX, and XII reported in Table 1 clearly indicated selective inhibition activity for the isoform II, thus suggesting an extensive range of potential biomedical applications for our compounds.

X-ray Crystallography. The X-ray crystal structures of hCA II in adduct with inhibitors **7c**, **11f**, and **11g** were determined at 1.55, 1.43, and 1.30 Å resolution, respectively, with the aim to establish the major interactions occurring between the amino acid residues lining the enzyme active site and the corresponding ligands (Figure 2A−F and Tables S2−S4 in the Supporting

https://doi.org/10.1021/acs.jmedchem.1c01906
J. Med. Chem. 2022, 65, 824−837

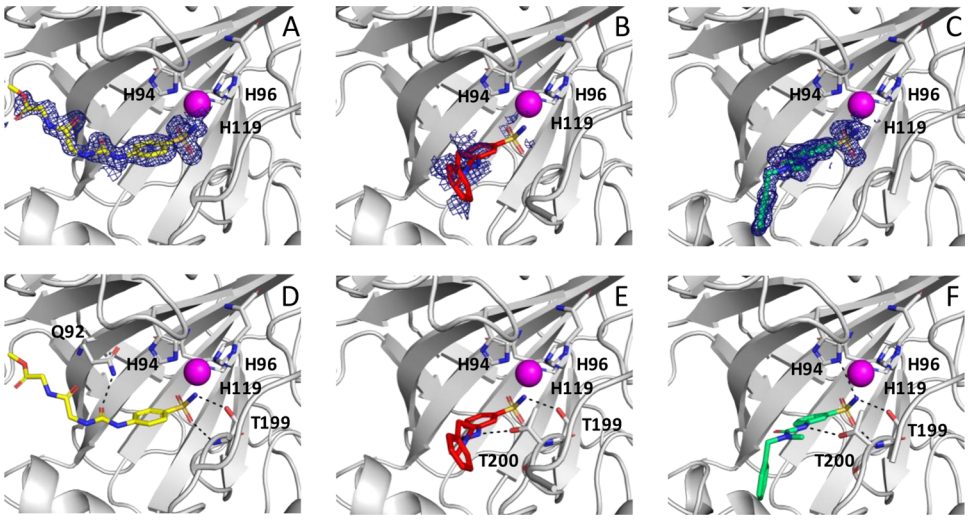

Figure 2. hCA II (gray) is depicted with the inhibitors **7c** (PDB 7RNZ) shown in yellow (A); **11f** (PDB 7ASJ) shown in red (B) and **11g** (PDB 7RNY) shown in green (C) are bound within the active site. The blue mesh is the density carved to 1.5 with a signal-to-noise ratio of 1.0. Protein residues (H94, H96, and H119) are shown by a stick model in CPK colors (labeled in panels (A−F)) and the zinc ion is shown by a magenta sphere. Residues involved in hydrogen bonding (black dashed lines) to their respective compounds are shown with the same color patterns as described above and labeled as such (panels D−F). In particular, (D) hydrogen bonds with Q92 and T199, (E) hydrogen bonds with T199 and T200, and (F) hydrogen bond formation with H94, T199, and T00.

Information). An overall inspection of the obtained structures showed **7c**, **11f**, and **11g** buried deep within the enzyme, with the primary sulfonamide anchored to the zinc metal ion according to the canonical binding cluster typical of the α-hCAs.[24]

Surprisingly, the conformationally unrestricted Gly-Gly-OMe moiety in **7c** was firmly stabilized within the hCA II pocket as revealed by the well-defined electron density of the corresponding adduct in Figure 2A. The molecular tail was flipped over the hydrophilic enzymatic half and secured by means of an intricate network of direct or water-mediated hydrogen bonds, specifically with Q92 and T199 (Figure 2D). Additionally, **7c** formed van der Waals interactions with E69, I91, V121, F131, V143, L198, T200, and W209 amino acid residues. A less defined electron density was reported for the distal section of the ligand for the hCA II/**11f** complex (Figure 2B), thus suggesting sustained ring flipping as expected from a conformationally unrestricted molecule. The major interactions taking part in the stabilization of the adduct are due to the hydrophobic bonds occurring between the sulfonamide aryl-containing group with V121 and L198 residues, and hydrogen bonds among the proximal ureidic nitrogen bond with T200, a hydrogen bond with T199, and the π-stacking of the terminal phenyl ring bond with W5. The van der Waals interactions with H4, V143, L198, P201, P202, and W209 also stabilize **11f**. As for the hCA II/**11g** adduct shown in Figure 2C, the ureido tail of the ligand showed preferential orientation toward the lipophilic half of the enzymatic cleft and was locked in place by means of either a hydrogen bond established between the distal ureido nitrogen with T200 or T-shaped π-stacking among the benzyl moiety with W5 (Figure 2C). The nitrogen following the benzensulfonamide in **11g** formed hydrogen bonds with H94, T199, and T200 (Figure 2F). Additionally, **11g** formed van der Waals interactions with V121, V143, L198, P201, P202, and W209.

Inhibitors **7c**, **11f**, and **11g** were overlayed within hCA II (Figure 3A). A zoomed-in view of this image showed that **7c** was bound further into the hydrophilic pocket than the other two compounds (Figure 3B). Despite the abundance of hydrogen

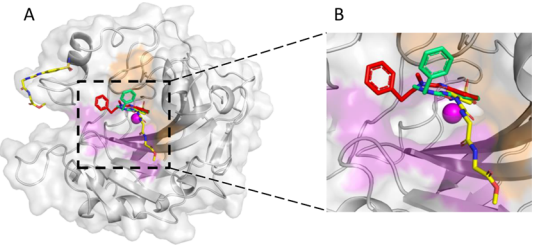

Figure 3. (A) Surface view overlayed onto a cartoon backbone of the entire hCA II (gray) enzyme bound with inhibitors **7c** (yellow), **11f** (red), and **11g** (green). The hydrophobic (orange) pocket and hydrophilic (purple) pocket are shaded as is the zinc atom (magenta sphere). All three compounds are bound to zinc within the active site. (B) Zoomed-in view of panel (A) to better observe the inhibitor modes of binding.

interactions in hCA II/**7c** compared to the hCA II/**11f/g** adducts, the inhibition data in Table 1 were in favor of the latter (K_I values of 45.3 and 1.6 and 9.3 nM, respectively). Such a result is reasonably justified when hydrophobic contacts are mainly used to determine the ligand−protein interactions such as for the hCA II/**11f/g** complexes.

Intraocular Pressure (IOP) Studies. The ability of the most potent hCA II inhibitors (i.e., compounds **7c**, **9c**, **11g**, and **12c**) to lower the IOP was assessed in hypertensive glaucomatous rabbits and compared to the effects induced by the commercially available drug dorzolamide (**DRZ**). In addition to the robust hCA II inhibition values observed in the selected compounds, the corresponding LogP values were also considered as inclusion criteria as optimal values are required in order to attain appropriate permeation across dynamic as well as static lipophilic ocular barriers. **7c**, **9c**, **11g**, and **12c** showed calculated LogP consensus values of −0.78, 1.26, 1.32, and 1.43, respectively, and thus inclusive of the **DRZ** LogP value of 0.85. All compounds were topically administered as eye drops at 1% w/v concentration, and a vehicle solution composed of 0.9% NaCl, 0.1% dimethyl sulfoxide (DMSO), and 0.1% EtOH was used as a control. The animals were pretreated

https://doi.org/10.1021/acs.jmedchem.1c01906
J. Med. Chem. 2022, 65, 824−837

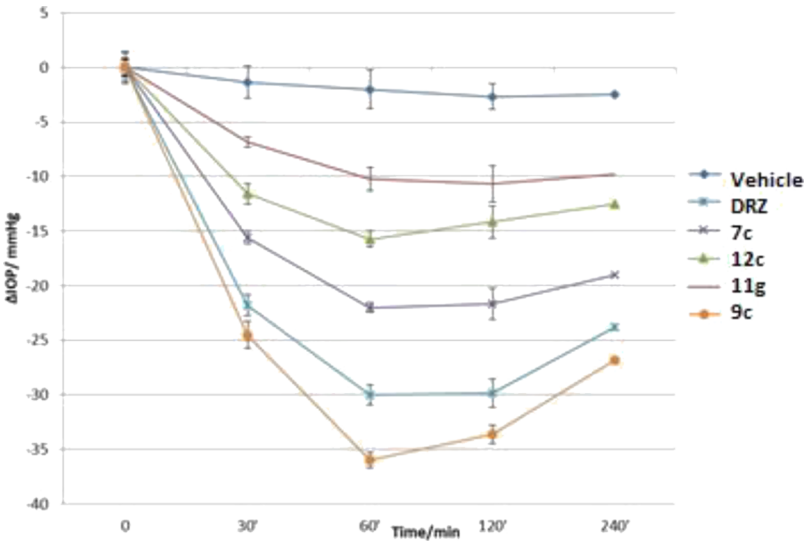

Figure 4. Plot of ΔIOP (mmHg) versus time (min) in hypertensive rabbit eyes treated with 50 μL of 1% solution of either **7c**, **9c**, **11g**, or **12c** and **DRZ** as the standard drug. Errors were in the range of 10−15% of the reported IOP values (from three different measurements for each of the four animals in the study group) and were statistically significant (p = 0.045, by Student's t-test).

by injection of 0.1 mL of 0.2% carbomer into the anterior chamber of both eyes to induce stable ocular hypertension (55 mmHg). Data in Figure 4 showed that all selected CAIs **7c**, **9c**, **11g**, and **12c** induce appreciable IOP reduction well over 4 h.

Significant ΔIOP reductions were observed when the ureido sulfanilamides **7c** and **9c** were administered. The Gly-Gly-OMe derivative **7c** showed a similar activity profile to the reference **DRZ** although being 1.3-fold less potent. It exhibited the maximum effect at 60 min postadministration, which lasted up to 120 min. Then, a slight increase of the ΔIOP values was observed, which, however, still accounted for an evident biological effect up to the end of the experimental time frame (ΔIOP −19 mmHg at 240 min). The (±) aspartate methyl ester **9c** induced stronger IOP reductions compared to **7c** for the entire experiment, as expected from its in vitro kinetic values, which accounted for lower hCA II inhibition values (i.e., K_I values of 3.6 and 45.3 nM for **9c** and **7c**, respectively). As shown in Figure 4, compound **9c** reached its maximal activity at 60 min postadministration with a ΔIOP value of −36 mmHg, thus 1.2-fold more potent than the reference drug **DRZ** at the same time point. The IOP reduction induced by **9c** gradually diminished up to the end of the experiment (i.e., 4 h) although its value was stronger compared to the reference **DRZ** (ΔIOP values of −27 and −24 mmHg for **9c** and **DRZ**, respectively). As for the metanilamide derivatives **11g** and **12c**, appreciable IOP reductions were induced although they were far less effective compared to the sulfanilamides **7c** and **9c** and the reference **DRZ** (Figure 4). Maximum effects were reported at 60 and 120 min postadministration for **11g** and **12c**, with ΔIOP values of −11 and −16 mmHg, respectively. Quite interestingly, remarkable differences in the induced IOP effects were observed for the regioisomers **9c** and **12c**, which were twice as much potent than their metanilamide counterpart. Such an effect may be attributed to the preferential binding to the hCA II isoform of **9c** compared to **12c** as reported in Table 1.

CONCLUSIONS

We reported a one-pot reaction procedure for the synthesis of asymmetrical ureidobenzenesulfonamides based on efficient in situ generation of the corresponding isocyanatobenzenesulfonamide species, followed by trapping with appropriate amines. Compounds of sulfanilamide **1a** and metanilamide **1b** series were synthesized in good yields and then were evaluated in vitro for their inhibitory profiles against four CA isoforms of biomedical interest (i.e., the hCAs I, II, IX, and XII). Overall, the compounds showed preferential inhibition of the hCA II isoform, with **10c** and **10d** being the most potent inhibitors (K_I values of 1.3 and 0.89 nM, respectively). The kinetic data observations were supported by the X-ray crystallographic studies of **7c**, **11f**, and **11g** in adduct with the hCA II isoform. All three complexes showed a high level of ordered electron density for the compounds within the active site, signifying reliable structural interpretation of their interactions. Since hCA II is deeply implicated in an abnormal increase of intraocular pressure in humans, we selected **9c**, **7c**, **11g**, and **12c** which exhibited different selectivity profiles for hCA II with K_I values spanning between 3.6 and 172.8 nM for evaluation of their IOP-lowering effect in comparison with **DRZ** as the standard. Compound **9c** showed the strongest lowering effect among the set with a ΔIOP reduction of around 36 mmHg. In addition, **9c** proved more potent than **DRZ** at the same concentration and retained the effect far over the experimental time of 240 min. We are confident that the data presented in this study present a convenient synthetic procedure for the production of ureido-containing compounds that will be beneficial and highly valuable for biomedical applications.

EXPERIMENTAL SECTION

Materials and Methods. *Chemistry.* All anhydrous solvents and reagents used in this study were purchased from Alfa Aesar, TCI, and Sigma-Aldrich. The synthetic reactions involving air- or moisture-sensitive chemicals were carried out under a nitrogen atmosphere using dried glassware and syringe to transfer the solutions. NMR (^{1}H-, ^{13}C-, and ^{19}F-NMR) spectra were recorded using a Bruker Advance III 400 MHz spectrometer using DMSO-d_6 as the solvent. The chemical shifts are reported in parts per million (ppm), and the coupling constants (J) are expressed in Hertz (Hz). The splitting patterns are denoted as s, singlet; d, doublet; t, triplet; q, quartet; m, multiplet; brs, broad singlet; and dd, doublet of doublets. The correct assignment of exchangeable protons (i.e., OH and NH) was carried out by means of the addition of D_2O. Analytical thin-layer chromatography (TLC) was carried out on

https://doi.org/10.1021/acs.jmedchem.1c01906
J. Med. Chem. 2022, 65, 824−837

Merck silica gel F-254 plates. Flash chromatography was performed using Merck silica gel 60 (230−400 mesh ASTM) as the stationary phase, and appropriate mixtures of ethyl acetate/*n*-hexane were used as the eluents. Melting points (m.p.) were measured in open capillary tubes with a Gallenkamp MPD350.BM3.5 apparatus and were uncorrected. The purity of the final compounds was determined using an Agilent 1200 liquid chromatography system composed of a autosampler, binary pumps, a column oven, and a diode-array detector (HPLC-DAD) operating in the UV range (210−400 nm). The operating conditions are reported in the Supporting Information. All compounds studied here were ≥95% HPLC pure. An HRMS analysis was performed with a Thermo Finnigan LTQ Orbitrap mass spectrometer coupled with an electrospray ionization source (ESI). The analysis was carried out in the positive ion mode $[M + H]^+$, and a proper dwell time acquisition was used to achieve 60,000 units of resolution at full width at half maximum. The elemental composition of the compounds was determined on the basis of their measured accurate masses, accepting only results with an attribution error less than 5 ppm and not an integer RDB (double bond/ring equivalents) value. Stock solutions of analytes were prepared using acetone (1.0 mg mL^{-1}) and stored at 4 °C. Then, the working solutions of each analyte were prepared by dilution of the stock solutions using Milli-Q H_2O/acetonitrile 1/1 (v/v) up to a concentration of 1.0 $\mu g\ mL^{-1}$. The HRMS analysis was performed by introducing the analyte working solution via a syringe pump at 10 $\mu L\ min^{-1}$. The solvents used in HPLC-DAD and HRMS measurements were acetone, acetonitrile (Chromasolv grade), and Milli-Q water of 18 MΩ cm.

General Procedure for Compounds 7a−c, 8, 9a−d, 10a−h, 11a−h, and 12a−e. A 2.0 M solution of aminobenzenesulfonamide **1a**/**1b** (1.0 equiv) in dry ACN at 0 °C was treated with TEA (5.0 equiv) followed by dropwise addition of a 20% v/v solution of phosgene in toluene (1.5 equiv). The reaction mixture was stirred at the same temperature for 5 min (a bright yellow color appeared) and the appropriate amine (**4a−h**, **5a−h**, **6a−e**, 2.0 equiv) was added and the reaction mixture was stirred until the starting material was consumed (TLC monitoring) and then quenched with slush and a 6.0 M aqueous solution of HCl. The formed precipitate was filtered-off, triturated with ethyl ether/petroleum ether, purified by silica gel column chromatography, and eluted with MeOH/DCM as eluents to afford the title compounds as solids.

*Synthesis of 4-(3-Isopropylureido)benzenesulfonamide (**7a**).* 4-(3-Isopropylureido)benzenesulfonamide **7a** was obtained according to the general procedure previously reported using 4-aminobenzenesulfonamide **1a** and isopropylamine **4a**. The crude compound was obtained after trituration from diethyl ether followed by silica gel column chromatography. Yield 53%; m.p. 214−215 °C; silica gel TLC R_f 0.31 (MeOH/DCM 10% v/v); δ_H (400 MHz, DMSO-d_6) 1.14 (6H, d, J = 6.8 Hz, $-(CH_3)_2$), 3.79 (1H, apt, J = 6.8 Hz, −CH), 6.19 (1H, d, J = 7.0 Hz, −CONH, exchange with D_2O), 7.19 (2H, s, SO_2NH_2, exchange with D_2O), 7.55 (2H, d, J = 9.2 Hz, Ar−H), 7.69 (2H, d, J = 8.8 Hz, Ar−H), 8.72 (1H, s, Ar−NHCO, exchange with D_2O); δ_C (100 MHz, DMSO-d_6) 23.9, 42.1, 117.7, 127.8, 137.0, 144.7, 155.1; ESI-HRMS (m/z) calculated for $[M + H]^+$ ion species $C_{10}H_{16}N_3O_3S$ 258.0907, found 258.0905.

*Synthesis of (±)-4-(3-(sec-Butyl)ureido)benzenesulfonamide (**7b**).* (±)-4-(3-(*sec*-Butyl)ureido)benzenesulfonamide **7b** was obtained according to the general procedure previously reported using 4-aminobenzenesulfonamide **1a** and (±)-*sec*-butyl amine **4b**. The crude compound was obtained after trituration from diethyl ether followed by silica gel column chromatography. Yield 61%; m.p. 212−213 °C; silica gel TLC R_f 0.33 (MeOH/DCM 10% v/v); δ_H (400 MHz, DMSO-d_6) 0.90 (3H, t, J = 6.0 Hz, $-CH_2CH_3$), 1.11 (3H, d, J = 6.0 Hz, $-CHCH_3$), 1.46 (2H, t, J = 6.0 Hz, $-CHCH_2CH_3$), 3.63 (1H, m, $-NHCHCH_2$), 6.15 (1H, d, J = 7.2 Hz, −CONHCH, exchange with D_2O), 7.18 (2H, s, SO_2NH_2, exchange with D_2O), 7.55 (2H, d, J = 8.0 Hz, Ar−H), 7.69 (2H, d, J = 8.0 Hz, Ar−H), 8.18 (1H, s, Ar−NHCO, exchange with D_2O); δ_C (100 MHz, DMSO-d_6) 11.1, 21.4, 30.1, 47.1, 117.5, 127.6, 136.8, 144.6, 155.2; ESI-HRMS (m/z) calculated for $[M + H]^+$ ion species $C_{11}H_{18}N_3O_3S$ 272.1063, found 272.1061.

*Synthesis of Methyl((4-sulfamoylphenyl)carbamoyl)-glycylglycinate (**7c**).* Methyl((4-sulfamoylphenyl)carbamoyl)-glycylglycinate **7c** was obtained according to the general procedure previously reported using 4-aminobenzenesulfonamide **1a** and glycylglycine methylester hydrochloride **4g**. The crude compound was obtained after trituration from diethyl ether followed by silica gel column chromatography. Yield 60%; m.p. 210−211 °C; silica gel TLC R_f 0.15 (MeOH/DCM 10% v/v); δ_H (400 MHz, DMSO-d_6) 3.64 (3H, s, $-OCH_3$), 3.81 (2H, d, J = 5.6 Hz, $-NHCH_2CO$), 3.88 (2H, d, J = 6.0 Hz, $-CH_2COOCH_3$), 6.52 (1H, t, J = 5.6 Hz, $-CONHCH_2$, exchange with D_2O), 7.16 (2H, s, SO_2NH_2, exchange with D_2O), 7.54 (2H, d, J = 8.8 Hz, Ar−H), 7.68 (2H, d, J = 8.4 Hz, Ar−H), 8.42 (1H, t, J = 6.0 Hz, $CONHCH_2$, exchange with D_2O), 9.19 (1H, s, Ar−NHCO, exchange with D_2O); δ_C (100 MHz, DMSO-d_6) 41.5, 43.3, 52.7, 117.8, 127.7, 137.2, 144.4, 155.7, 170.9, 171.2; ESI-HRMS (m/z) calculated for $[M + H]^+$ ion species $C_{12}H_{17}N_4O_6S$ 345.0863, found 345.0864.

*Synthesis of 4-(3,3-Dimethylureido)benzenesulfonamide (**8**).* 4-(3,3-Dimethylureido)benzenesulfonamide **8** was obtained according to the general procedure previously reported using 4-aminobenzenesulfonamide **1a** and *N*,*N*-dimethylamine hydrochloride **5i**. The crude compound was obtained after trituration from ethyl ether followed by silica gel column chromatography. Yield 63%; m.p. 250−251 °C; silica gel TLC R_f 0.35 (MeOH/DCM 10% v/v); δ_H (400 MHz, DMSO-d_6) 2.98 (6H, s, $-N(CH_3)_2$), 7.19 (2H, s, SO_2NH_2, exchange with D_2O), 7.66 (2H, d, J = 9.2 Hz, Ar−H), 7.7 (2H, d, J = 8.8 Hz, Ar−H), 8.67 (1H, s, Ar−NHCO, exchange with D_2O); δ_C (100 MHz, DMSO-d_6) 37.3, 119.6, 127.3, 137.5, 145.0, 156.4; ESI-HRMS (m/z) calculated for $[M + H]^+$ ion species $C_9H_{14}N_3O_3S$ 244.0750, found 244.0749.

*Synthesis of Methyl((4-sulfamoylphenyl)carbamoyl)glycinate (**9a**).* Methyl((4-sulfamoylphenyl)carbamoyl)glycinate **9a** was obtained according to the general procedure previously reported using 4-aminobenzenesulfonamide **1a** and glycine methylester hydrochloride **6a**. The crude compound was obtained after trituration from diethyl ether followed by silica gel column chromatography. Yield 64%; m.p. 214−215 °C; silica gel TLC R_f 0.38 (MeOH/DCM 10% v/v); δ_H (400 MHz, DMSO-d_6) 3.69 (3H, s, $-OCH_3$), 3.93 (2H, d, J = 6.0 Hz, $-NHCH_2COOCH_3$), 6.65 (1H, t, J = 6.0 Hz, CH_2NHCO, exchange with D_2O), 7.20 (2H, s, SO_2NH_2, exchange with D_2O), 7.58 (2H, d, J = 8.8 Hz, Ar−H), 7.71 (2H, d, J = 8.8 Hz, Ar−H), 9.25 (1H, s, Ar−NHCO, exchange with D_2O); δ_C (100 MHz, DMSO-d_6) 42.3, 52.7, 118.0, 127.8, 137.4, 144.4, 155.9, 172.2; ESI-HRMS (m/z) calculated for $[M + H]^+$ ion species $C_{10}H_{14}N_3O_5S$ 288.0649, found 288.0646.

*Synthesis of (±)-Methyl((4-sulfamoylphenyl)carbamoyl)-leucinate (**9b**).* (±)-Methyl((4-sulfamoylphenyl)carbamoyl)leucinate **9b** was obtained according to the general procedure previously reported using 4-aminobenzenesulfonamide **1a** and (±)-leucine methylester hydrochloride **6b**. The crude compound was obtained after trituration from diethyl ether followed by silica gel column chromatography. Yield 68%; m.p. 179−180 °C; silica gel TLC R_f 0.40 (MeOH/DCM 10% v/v); δ_H (400 MHz, DMSO-d_6) 0.9 (6H, t, J = 6.4 Hz, $-CH(CH_3)_2$), 1.55 (2H, t, J = 5.6 Hz, $-CHCH_2CH(CH_3)_2$), 1.66 (1H, m, $-NHCHCH_2$), 3.66 (3H, s, $-OCH_3$), 4.27 (1H, q, J = 6.4 Hz, $-NHCH(CH_3)_2$), 6.70 (1H, d, J = 8.0 Hz, −CONHCH, exchange with D_2O), 7.17 (2H, s, SO_2NH_2, exchange with D_2O), 7.53 (2H, d, J = 8.8 Hz, Ar−H), 7.68 (2H, d, J = 8.8 Hz, Ar−H), 8.94 (1H, s, Ar−NHCO, exchange with D_2O); δ_C (100 MHz, DMSO-d_6) 22.4, 23.6, 25.3, 41.4, 51.7, 52.8, 117.8, 127.7, 137.4, 144.0, 155.4, 174.5; ESI-HRMS (m/z) calculated for $[M + H]^+$ ion species $C_{14}H_{22}N_3O_5S$ 344.1275, found 344.1273.

*Synthesis of (±)-Methyl((4-sulfamoylphenyl)carbamoyl) phenyl-alaninate (**9c**).* (±)-Methyl((4-sulfamoylphenyl)carbamoyl)-phenylalaninate **9c** was obtained according to the general procedure previously reported using 4-aminobenzenesulfonamide **1a** and (±)-phenylalanine methylester hydrochloride **6c**. The crude compound was obtained after trituration from diethyl ether followed by silica gel column chromatography. Yield 62%; m.p. 200−201 °C; silica gel TLC R_f 0.52 (MeOH/DCM 10% v/v); δ_H (400 MHz, DMSO-d_6) 3.1 (2H, m, $CHCH_2Ar$), 3.69 (3H, s, $-OCH_3$), 4.57 (1H, m, $NHCHCH_2$), 6.65 (1H, d, J = 7.6 Hz, −NHCH, exchange with D_2O), 7.2 (2H, s, SO_2NH_2, exchange with D_2O), 7.30 (5H, m, Ar−H), 7.53 (2H, d, J = 8.8 Hz, Ar−H), 7.7 (2H, d, J = 8.8 Hz, Ar−H), 9.11 (1H, s,

https://doi.org/10.1021/acs.jmedchem.1c01906
J. Med. Chem. 2022, 65, 824−837

Ar−NH, exchange with D_2O); δ_C (100 MHz, DMSO-d_6) 38.3, 53.0, 54.8, 118.0, 127.7, 127.8, 129.4, 130.2, 137.5, 137.8, 144.1, 155.3, 173.5; ESI-HRMS (m/z) calculated for $[M + H]^+$ ion species $C_{17}H_{20}N_3O_5S$ 378.1118, found 378.1118.

*Synthesis of (±)-Dimethyl((4-sulfamoylphenyl)carbamoyl)-glutamate (**9d**).* (±)-Dimethyl((4-sulfamoylphenyl)carbamoyl)-glutamate **9d** was obtained according to the general procedure previously reported using 4-aminobenzenesulfonamide **1a** and (±)-glutamic acid dimethylester hydrochloride **6d**. The crude compound was obtained after trituration from diethyl ether followed by silica gel column chromatography. Yield 59%; m.p. 174−175 °C; silica gel TLC R_f 0.13 (MeOH/DCM 10% v/v); δ_H (400 MHz, DMSO-d_6) 2.0 (2H, m, $-CHCH_2CH_2$), 2.4 (2H, m, $-CHCH_2CH_2$), 3.60 (3H, s, $-OCH_3$), 3.67 (3H, s, $-OCH_3$), 4.29 (2H, q, J = 5.2 Hz, $-NHCHCH_2$), 6.77 (1H, d, J = 8.0 Hz, −CONHCH, exchange with D_2O), 7.19 (2H, s, SO_2NH_2, exchange with D_2O), 7.53 (2H, d, J = 8.8 Hz, Ar−H), 7.68 (2H, d, J = 8.8 Hz, Ar−H), 9.0 (1H, s, Ar−NHCO, exchange with D_2O); δ_C (100 MHz, DMSO-d_6) 27.8, 52.5, 52.7, 53.1, 118.1, 127.8, 137.6, 144.1, 155.5, 173.6, 173.7, 198.3; ESI-HRMS (m/z) calculated for $[M + H]^+$ ion species $C_{14}H_{20}N_3O_7S$ 374.1017, found 374.1020.

*Synthesis of 3-(3-Isopropylureido)benzenesulfonamide (**10a**).* 3-(3-Isopropylureido)benzenesulfonamide **10a** was obtained according to the general procedure previously reported using 3-aminobenzenesulfonamide **1b** and isopropylamine **4a**. The crude compound was obtained after trituration from diethyl ether followed by silica gel column chromatography. Yield 65%; m.p. 205−206 °C; silica gel TLC R_f 0.45 (MeOH/DCM 10% v/v); δ_H (400 MHz, DMSO-d_6) 1.11 (6H, d, J = 6.4 Hz, 2× $-CH(CH_3)_2$), 3.77 (1H, m, 2× $-NCH(CH_3)_2$), 6.06 (1H, d, J = 7.6 Hz, CONHCH, exchange with D_2O), 7.30 (2H, s, SO_2NH_2, exchange with D_2O), 7.32−7.48 (3H, m, Ar−H), 7.98 (1H, s, Ar−H), 8.63 (1H, s, Ar−NH, exchange with D_2O); δ_C (100 MHz, DMSO-d_6) 23.9, 42.1, 115.5, 119.0, 121.4, 130.3, 142.0, 145.6, 155.3; ESI-HRMS (m/z) calculated for $[M + H]^+$ ion species $C_{10}H_{16}N_3O_3S$ 258.0907, found 258.0905.

*Synthesis of (±)-3-(3-(sec-Butyl)ureido)benzenesulfonamide (**10b**).* (±)-3-(3-(*sec*-Butyl)ureido)benzenesulfonamide **10b** was obtained according to the general procedure previously reported using 3-aminobenzenesulfonamide **1b** and (±)-*sec*-butylamine **4b**. The crude compound was obtained after trituration from diethyl ether followed by silica gel column chromatography. Yield 60%; m.p. 139−140 °C; silica gel TLC R_f 0.47 (MeOH/DCM 10% v/v); δ_H (400 MHz, DMSO-d_6) 3.64 (1H, m, −NHCH), 6.06 (1H, d, J = 8.4 Hz, CONHCH, exchange with D_2O), 7.32 (2H, s, SO_2NH_2, exchange with D_2O), 7.36−7.51 (3H, m, Ar−H), 8.02 (1H, s, Ar−H), 8.66 (1H, s, Ar−NH, exchange with D_2O); δ_C (100 MHz, DMSO-d_6) 11.4, 21.7, 30.3, 47.3, 115.4, 119.0, 121.4, 130.3, 142.1, 145.6, 155.5; ESI-HRMS (m/z) calculated for $[M + H]^+$ ion species $C_{11}H_{18}N_3O_3S$ 272.1063, found 272.1063.

*Synthesis of 3-(3-Phenethylureido)benzenesulfonamide (**10c**).* 3-(3Phenethylureido)benzenesulfonamide **10c** was obtained according to the general procedure previously reported using 3-aminobenzenesulfonamide **1b** and phenethylamine **4c**. The crude compound was obtained after trituration from diethyl ether followed by silica gel column chromatography. Yield 41%; m.p. 149−150 °C; silica gel TLC R_f 0.53 (MeOH/DCM 10% v/v); δ_H (400 MHz, DMSO-d_6) 2.09 (2H, t, J = 7.6 Hz, $-CH_2CH_2Ar$), 3.35 (2H, q, J = 7.6 Hz, $-NHCH_2CH_2$), 6.20 (1H, t, J = 6.0 Hz, $-CONHCH_2$, exchange with D_2O), 7.22 (5H, m, Ar−H), 7.26 (2H, brs, SO_2NH_2, exchange with D_2O), 7.41 (3H, m, Ar−H), 7.99 (1H, s, Ar−H), 8.85 (1H, s, Ar−NHCO, exchange with D_2O); δ_C (100 MHz, DMSO-d_6) 36.8, 41.7, 115.5, 119.1, 121.4, 127.2, 129.5, 129.7, 130.3, 140.6, 142.0, 145.6, 155.9; ESI-HRMS (m/z) calculated for $[M + H]^+$ ion species $C_{15}H_{18}N_3O_3S$ 320.1063, found 320.1064.

*Synthesis of 3-(3-Phenylureido)benzenesulfonamide (**10d**).* 3-(3-Phenylureido)benzenesulfonamide **10d** was obtained according to the general procedure previously reported using 3-aminobenzenesulfonamide **1b** and aniline **4d**. The crude compound was obtained after trituration from diethyl ether followed by silica gel column chromatography. Yield 59%; m.p. 233−235 °C; silica gel TLC R_f 0.52 (MeOH/DCM 10% v/v); δ_H (400 MHz, DMSO-d_6) 6.97 (1H, appt, J = 6.4, Ar−H), 7.28−7.57 (9H, m, Ar−H and SO_2NH_2, exchange with D_2O), 8.08 (1H, s, Ar−H), 8.73 (1H, s, CONHAr, exchange with D_2O), 9.01 (1H, s, Ar−NHCO, exchange with D_2O). δ_C (100 MHz, DMSO-d_6) 116.1, 119.4, 119.9, 122.1, 123.2, 140.5, 141.2, 145.8, 153.5; ESI-HRMS (m/z) calculated for $[M + H]^+$ ion species $C_{13}H_{14}N_3O_3S$ 292.0750, found 292.0750.

*Synthesis of 3-(3-(2-Fluorophenyl)ureido)benzenesulfonamide (**10e**).* 3-(3-(2-Fluorophenyl)ureido)benzenesulfonamide **10e** was obtained according to the general procedure previously reported using 3-aminobenzenesulfonamide **1b** and 2-fluoroaniline **4e**. The crude compound was obtained after trituration from diethyl ether followed by silica gel column chromatography. Yield 67%; m.p. 191−192 °C; silica gel TLC R_f 0.45 (MeOH/DCM 10% v/v); δ_H (400 MHz, DMSO-d_6) 7.35 (1H, m, Ar−H), 7.37 (2H, s, SO_2NH_2, exchange with D_2O), 7.53 (5H, m, Ar−H), 8.05 (1H, m, Ar−H), 8.10 (1H, d, J = 1.7 Hz, Ar−H), 9.11 (1H, s, NHCONH, exchange with D_2O), 9.15 (1H, s, NHCONH, exchange with D_2O); δ_C (100 MHz, DMSO-d_6) 116.0, 120.2, 121.8, 122.0, 123.8 (J = 28 Hz), 125.6, 128.3, 128.4, 130.6, 140.9, 145.9, 153.1 (J = 240 Hz), 153.14; δ_F (376 MHz, DMSO-d_6), −129.7 (3F, s); ESI-HRMS (m/z) calculated for $[M + H]^+$ ion species $C_{13}H_{13}FN_3O_3S$ 310.0656, found 310.0659.

*Synthesis of 3-(3-(3-(Trifluoromethyl)phenyl)ureido)-benzenesulfonamide (**10f**).* 3-(3-(3-(Trifluoromethyl)phenyl)ureido)-benzenesulfonamide **10f** was obtained according to the general procedure previously reported using 3-aminobenzenesulfonamide **1b** and 3-(trifluoromethyl)-aniline **4f**. The crude compound was obtained after trituration from diethyl ether followed by silica gel column chromatography. Yield 44%; m.p. 289−290 °C; silica gel TLC R_f 0.32 (MeOH/DCM 10% v/v); δ_H (400 MHz, DMSO-d_6) 7.33−7.61 (9H, m, Ar−H and SO_2NH_2, exchange with D_2O), 8.05 (1H, s, Ar−H), 8.11 (1H, s, Ar−H), 9.11 (1H, s, Ar−NH, exchange with D_2O), 9.15 (1H, s, Ar−NH, exchange with D_2O); δ_C (100 MHz, DMSO-d_6) 115.3, 116.3, 119.3, 122.3, 123.8, 125.2 (J = 270 Hz), 130.3 (J = 32 Hz), 130.4, 130.7, 131.0, 140.8, 141.3, 145.7, 153.4; δ_F (376 MHz, DMSO-d_6) −61.3 (1F, s); ESI-HRMS (m/z) calculated for $[M + H]^+$ ion species $C_{14}H_{13}F_3N_3O_3S$ 360.0624, found 360.0621.

*Synthesis of Methyl((3-sulfamoylphenyl)carbamoyl)-glycylglycinate (**10g**).* Methyl((3-sulfamoylphenyl)carbamoyl)-glycylglycinate **10g** was obtained according to the general procedure previously reported using 3-aminobenzenesulfonamide **1b** and glycylglycine methyl ester hydrochloride **4g**. The crude compound was obtained after trituration from diethyl ether followed by silica gel column chromatography. Yield 41%; m.p. 70−71 °C; silica gel TLC R_f 0.19 (MeOH/DCM 10% v/v); δ_H (400 MHz, DMSO-d_6) 3.64 (3H, s, $-OCH_3$), 3.81 (2H, d, J = 5.6 Hz, $-NHCH_2COO$), 3.89 (2H, d, J = 5.6 Hz, $-NHCH_2CO$), 6.46 (1H, t, J = 5.6 Hz, $CONHCH_2$, exchange with D_2O), 7.31 (2H, s, SO_2NH_2, exchange with D_2O), 7.34−7.54 (3H, m, Ar−H), 7.99 (1H, s, Ar−H), 8.41 (1H, t, J = 6.0 Hz, $CONHCH_2$, exchange with D_2O), 9.12 (1H, s, Ar−NH, exchange with D_2O); δ_C (100 MHz, DMSO-d_6) 41.6, 43.4, 52.8, 115.5, 119.3, 121.5, 130.3, 141.8, 145.7, 156.0, 171.1, 171.3; ESI-HRMS (m/z) calculated for $[M + H]^+$ ion species $C_{11}H_{15}N_4O_6S$ 331.0707, found 331.0709.

*Synthesis of Methyl 4-(3-(3-sulfamoylphenyl)ureido)butanoate (**10h**).* Methyl 4-(3-(3-sulfamoylphenyl)ureido)butanoate **10h** was obtained according to the general procedure previously reported using 3-aminobenzenesulfonamide **1b** and γ-aminobutyric acid (GABA) methylester hydrochloride **4h**. The crude compound was obtained after trituration from diethyl ether followed by silica gel column chromatography. Yield 73%; m.p. 142−143 °C; silica gel TLC R_f 0.63 (MeOH/DCM 10% v/v); δ_H (400 MHz, DMSO-d_6) 1.70 (2H, m, $-CH_2-$), 2.35 (2H, t, J = 7.6 Hz, $-CH_2COO$), 3.12 (2H, t, J = 5.6 Hz, $-NHCH_2$), 3.60 (3H, s, $-OCH_3$), 6.26 (1H, t, J = 5.6, CONH, exchange with D_2O), 7.29 (2H, s, SO_2NH_2, exchange with D_2O), 7.33−7.42 (2H, m, Ar−H), 7.50−7.53 (1H, m, Ar−H), 7.98 (1H, s, Ar−H), 8.78 (1H, s, Ar−NH, exchange with D_2O); δ_C (100 MHz, DMSO-d_6) 26.2, 31.8, 39.5, 52.3, 115.6, 119.0, 121.5, 130.3, 142.0, 145.6, 156.1, 174.2; ESI-HRMS (m/z) calculated for $[M + H]^+$ ion species $C_{12}H_{18}N_3O_5S$ 316.0962, found 316.0960.

*Synthesis of 3-(3,3-Diethylureido)benzenesulfonamide (**11a**).* 3-(3,3-Diethylureido)benzenesulfonamide **11a** was obtained according

https://doi.org/10.1021/acs.jmedchem.1c01906
J. Med. Chem. 2022, 65, 824−837

to the general procedure previously reported using 3-aminobenzenesulfonamide **1b** and diethylamine **5a**. The crude compound was obtained after trituration from diethyl ether followed by silica gel column chromatography. Yield 60%; m.p. 155−156 °C; silica gel TLC R_f 0.62 (MeOH/DCM 10% v/v); δ_H (400 MHz, DMSO-d_6) 1.10 (6H, t, J = 6.8 Hz, 2× $-CH_3$), 3.40 (4H, q, J = 6.8 Hz, $-NCH_2-$), 7.28 (2H, s, SO_2NH_2, exchange with D_2O), 7.39 (2H, m, Ar−H), 7.72 (1H, dt, J = 7.2 Hz, 2.0 Hz, Ar−H), 8.1 (1H, s, Ar−H), 8.5 (1H, s, Ar−NH, exchange with D_2O); δ_C (100 MHz, DMSO-d_6) 14.9, 41.7, 117.8, 119.6, 123.6, 129.8, 142.3, 145.2, 155.3; ESI-HRMS (m/z) calculated for $[M + H]^+$ ion species $C_{11}H_{18}N_3O_3S$ 272.1063, found 272.1064.

*Synthesis of 3-(3,3-Dipropylureido)benzenesulfonamide (**11b**).* 3-(3,3-Dipropylureido)benzenesulfonamide **11b** was obtained according to the general procedure previously reported using 3-aminobenzenesulfonamide **1b** and dipropylamine **5b**. The crude compound was obtained after trituration from diethyl ether followed by silica gel column chromatography. Yield 54%; m.p. 131−132 °C; silica gel TLC R_f 0.55 (MeOH/DCM 10% v/v); δ_H (400 MHz, DMSO-d_6) 0.9 (6H, t, J = 7.2 Hz, 2× $-CH_3$), 1.56 (4H, m, 2× $-CH_2-$), 3.30 (4H, t, J = 7.6 Hz, 2× $-NCH_2-$), 7.31 (2H, s, SO_2NH_2, exchange with D_2O), 7.42 (2H, m, Ar−H), 7.72 (1H, dt, J = 7.2 Hz, 2.4 Hz, Ar−H), 8.10 (1H, s, Ar−H), 8.50 (1H, s, Ar−NHCO, exchange with D_2O); δ_C (100 MHz, DMSO-d_6) 12.2, 22.3, 49.0, 117.8, 119.6, 123.7, 129.8, 142.3, 145.2, 155.7; ESI-HRMS (m/z) calculated for $[M + H]^+$ ion species $C_{13}H_{22}N_3O_3S$ 300.1376, found 300.1375.

*Synthesis of 3-(3,3-Dihexylureido)benzenesulfonamide (**11c**).* 3-(3,3-Dihexylureido)benzenesulfonamide **11c** was obtained according to the general procedure previously reported using 3-aminobenzenesulfonamide **1b** and *N,N*-dihexylamine **5c**. The crude compound was obtained after trituration from diethyl ether followed by silica gel column chromatography. Yield 51%; m.p. 161−162 °C; silica gel TLC R_f 0.65 (MeOH/DCM 10% v/v); δ_H (400 MHz, DMSO-d_6) 0.89 (6H, t, J = 6.8 Hz, 2× $-CH_3$), 1.31 (12H, m, 2× $-CH_2CH_2CH_2$), 1.52 (4H, t, J = 6.8 Hz, 2× $-NCH_2CH_2$), 3.20 (4H, t, J = 6.8 Hz, 2× $-NCH_2CH_2$), 7.31 (2H, s, SO_2NH_2, exchange with D_2O), 7.39−7.45 (2H, m, Ar−H), 7.71 (1H, dt, J = 7.2 Hz, 2.0 Hz), 8.06 (1H, s, Ar−H), 8.49 (1H, s, Ar−NH, exchange with D_2O); δ_C (100 MHz, DMSO-d_6) 15.0, 23.1, 27.0, 29.1, 32.2, 47.4, 117.7, 119.6, 123.6, 129.8, 142.3, 145.2, 155.6; ESI-HRMS (m/z) calculated for $[M + H]^+$ ion species $C_{19}H_{34}N_3O_3S$ 384.2315, found 384.2318.

*Synthesis of 3-(3,3-Diisopropylureido)benzenesulfonamide (**11d**).* 3-(3,3-Diisopropylureido)benzenesulfonamide **11d** was obtained according to the general procedure previously reported using 3-aminobenzenesulfonamide **1b** and *N,N*-diisopropylamine **5d**. The crude compound was obtained after trituration from diethyl ether followed by silica gel column chromatography. Yield 47%; m.p. 165−166 °C; silica gel TLC R_f 0.59 (MeOH/DCM 10% v/v); δ_H (400 MHz, DMSO-d_6) 1.25 (12H, d, J = 6.8 Hz, 2× $-(CH_3)_2$), 3.84 (2H, m 2× $-CH-$), 7.26 (2H, s, $-SO_2NH_2$, exchange with D_2O), 7.37 (2H, m, Ar−H), 7.63 (1H, dt, J = 5.6 Hz, 1.6 Hz, Ar−H), 8.02 (1H, s, Ar−H), 8.40 (1H, s, Ar−NH, exchange with D_2O); δ_C (100 MHz, DMSO-d_6) 22.2, 46.8, 117.8, 119.3, 123.7, 129.7, 142.6, 145.1, 154.6; ESI-HRMS (m/z) calculated for $[M + H]^+$ ion species $C_{13}H_{22}N_3O_3S$ 300.1376, found 300.1374.

*Synthesis of 3-(3,3-Diisobutylureido)benzenesulfonamide (**11e**).* 3-(3,3-Diisobutylureido)benzenesulfonamide **11e** was obtained according to the general procedure previously reported using 3-aminobenzenesulfonamide **1b** and *N,N*-diisobutylamine **5e**. The crude compound was obtained after trituration from diethyl ether followed by silica gel column chromatography. Yield 50%; m.p. 109−110 °C; silica gel TLC R_f 0.50 (MeOH/DCM 10% v/v); δ_H (400 MHz, DMSO-d_6) 0.85 (12H, d, J = 6.8 Hz, 2× $-(CH_3)_2$), 1.92 (2H, m, −CH), 3.18 (4H, d, J = 7.2 Hz, 2× $-NCH_2$), 7.29 (2H, s, SO_2NH_2, exchange with D_2O), 7.39 (2H, m, Ar−H), 7.66 (1H, dt, J = 7.6 Hz, 2.0 Hz, Ar−H), 8.02 (1H, s, Ar−H), 8.51 (1H, s, Ar−NH, exchange with D_2O); δ_C (100 MHz, DMSO-d_6) 20.9, 28.0, 55.0, 117.6, 119.6, 123.5, 129.8, 142.3, 145.2, 156.4; ESI-HRMS (m/z) calculated for $[M + H]^+$ ion species $C_{15}H_{26}N_3O_3S$ 328.1689, found 328.1691.

*Synthesis 3-(3-Methyl-3-phenethylureido)benzenesulfonamide (**11f**).* 3-(3-Methyl-3-phenylureido)benzenesulfonamide **11f** was obtained according to the general procedure previously reported using 3-aminobenzenesulfonamide **1b** and *N*-methyl-aniline **5f**. The crude compound was obtained after trituration from diethyl ether followed by silica gel column chromatography. Yield 43%; m.p. 209−210 °C; silica gel TLC R_f 0.73 (MeOH/DCM 10% v/v); δ_H (400 MHz, DMSO-d_6) 2.52 (2H, m, $-CH_2$), 2.81 (2H, m, $-CH_2$), 3.30 (3H, s, $-CH_3$), 7.25−7.45 (9H, m, Ar−H and SO_2NH_2, exchange with D_2O), 7.67 (1H, m, Ar−H), 7.98 (1H, s, Ar−H), 8.51 (1H, s, Ar−NH, exchange with D_2O); δ_C (100 MHz, DMSO-d_6) 33.1, 38.7, 55.6, 117.8, 120.0, 123.6, 127.1, 127.5, 129.9, 130.3, 141.7, 144.9, 145.3, 155.6; ESI-HRMS (m/z) calculated for $[M + H]^+$ ion species $C_{16}H_{19}N_3O_3S$ 333.1147, found 333.1145.

*Synthesis of 3-(3-Benzyl-3-methylureido)benzenesulfonamide (**11g**).* 3-(3-Benzyl-3-methylureido)benzenesulfonamide **11g** was obtained according to the general procedure previously reported using 3-aminobenzenesulfonamide **1b** and *N*-methyl benzylamine **5g**. The crude compound was obtained after trituration from diethyl ether followed by silica gel column chromatography. Yield 50%; m.p. 158−159 °C; silica gel TLC R_f 0.30 (MeOH/DCM 10% v/v); δ_H (400 MHz, DMSO-d_6) 2.97 (3H, s, $-CH_3$), 4.61 (2H, s, $-NCH_2$), 7.29−7.46 (9H, m, Ar−H and SO_2NH_2, exchange with D_2O), 7.75 (1H, d, J = 7.6 Hz, Ar−H), 8.12 (1H, s, Ar−H), 8.81 (1H, s, Ar−NH, exchange with D_2O); δ_C (100 MHz, DMSO-d_6) 35.4, 52.3, 117.7, 119.8, 123.6, 128.1, 128.3, 129.6, 129.9, 139.2, 142.2, 145.3, 156.5; ESI-HRMS (m/z) calculated for $[M + H]^+$ ion species $C_{15}H_{18}N_3O_3S$ 320.1063, found 320.1064.

*Synthesis of N-(3-Sulfamoylphenyl)piperidine-1-carboxamide (**11h**).* *N*-(3-Sulfamoylphenyl)piperidine-1-carboxamide **11h** was obtained according to the general procedure previously reported using 3-aminobenzenesulfonamide **1b** and piperidine **5h**. The crude compound was obtained after trituration from diethyl ether followed by silica gel column chromatography. Yield 35%; m.p. 201−202 °C; silica gel TLC R_f 0.39 (MeOH/DCM 10% v/v); δ_H (400 MHz, DMSO-d_6) 1.50 (4H, m, $-CH_2$), 1.58 (2H, m, $-CH_2$), 3.34 (4H, m, 2× $-CH_2$), 7.28 (2H, s, SO_2NH_2, exchange with D_2O), 7.38 (2H, m, Ar−H), 7.66 (1H, m, Ar−H), 8.02 (1H, s, Ar−H), 8.77 (1H, s, Ar−NH, exchange with D_2O); δ_C (100 MHz, DMSO-d_6) 25.1, 26.6, 45.7, 117.4, 119.5, 123.2, 129.9, 142.4, 145.3, 155.6; ESI-HRMS (m/z) calculated for $[M + H]^+$ ion species $C_{12}H_{18}N_3O_3S$ 284.1063, found 284.1065.

*Synthesis of Methyl((3-sulfamoylphenyl)carbamoyl)glycinate (**12a**).* Methyl((3-sulfamoylphenyl)carbamoyl)glycinate **12a** was obtained according to the general procedure previously reported using 3-aminobenzenesulfonamide **1b** and glycine methyl ester hydrochloride **6a**. The crude compound was obtained after trituration from diethyl ether followed by silica gel column chromatography. Yield 40%; m.p. 174−175 °C; silica gel TLC R_f 0.44 (MeOH/DCM 10% v/v); δ_H (400 MHz, DMSO-d_6) 3.69 (3H, s, $-OCH_3$), 3.93 (2H, d, J = 5.4 Hz, $-CH_2COO$), 6.60 (1H, t, J = 5.4 Hz, −CONH), 7.34 (2H, s, SO_2NH_2, exchange with D_2O), 7.43 (2H, m, Ar−H), 7.55 (1H, d, J = 8.0 Hz, Ar−H), 8.04 (1H, s, Ar−H), 9.21 (1H, s, Ar−NH, exchange with D_2O); δ_C (100 MHz, DMSO-d_6) 42.4, 52.7, 115.7, 119.4, 121.6, 130.3, 141.7, 145.7, 156.1, 172.2; ESI-HRMS (m/z) calculated for $[M + H]^+$ ion species $C_{10}H_{14}N_3O_5S$ 288.0649, found 288.0646.

*Synthesis of (±)-Methyl((3-sulfamoylphenyl)carbamoyl)-leucinate (**12b**).* (±)-Methyl((3-sulfamoylphenyl)carbamoyl)-leucinate **12b** was obtained according to the general procedure previously reported using 3-aminobenzenesulfonamide **1b** and (±)-leucine methyl ester hydrochloride **6b**. The crude compound was obtained after trituration from petroleum ether followed by silica gel column chromatography. Yield 61%; m.p. 73−74 °C; silica gel TLC R_f 0.42 (MeOH/DCM 10% v/v); δ_H (400 MHz, DMSO-d_6) 0.91 (6H, t, J = 6.8 Hz, 2× $-(CH_3)_2$), 1.54 (2H, m, $-CH_2$), 1.65 (1H, m, −CH), 3.66 (3H, s, $-COOCH_3$), 4.27 (1H, m, −CH), 6.61 (1H, d, J = 8.0 Hz, −CONH, exchange with D_2O), 7.30 (2H, s, SO_2NH_2, exchange with D_2O), 7.35−7.46 (3H, m, Ar−H), 8.02 (1H, s, Ar−H), 8.88 (1H, s, Ar−NH, exchange with D_2O); δ_C (100 MHz, DMSO-d_6) 22.6, 23.8, 25.4, 41.6, 51.9, 53.0, 115.6, 119.5, 121.6, 130.4, 141.5, 145.7, 155.7, 174.7; ESI-HRMS (m/z) calculated for $[M + H]^+$ ion species $C_{14}H_{22}N_3O_5S$ 344.1275, found 344.1272.

https://doi.org/10.1021/acs.jmedchem.1c01906
J. Med. Chem. 2022, 65, 824−837

*Synthesis of (±)-Methyl((3-sulfamoylphenyl)carbamoyl)-phenylalaninate (**12c**).* (±)-Methyl((3-sulfamoylphenyl)carbamoyl)-phenylalaninate **12c** was obtained according to the general procedure previously reported using 3-aminobenzenesulfonamide **1b** and (±)-phenylalanine methyl ester hydrochloride **6c**. The crude compound was obtained after trituration from diethyl ether followed by silica gel column chromatography. Yield 55%; m.p. 83−84 °C; silica gel TLC R_f 0.50 (MeOH/DCM 10% v/v); δ_H (400 MHz, DMSO-d_6) 3.07 (2H, m, $-CH_2-$Ar), 4.56 (1H, m, −CH), 6.59 (1H, d, J = 8.0 Hz, −CONHCH), 7.23−7.49 (10H, m, Ar−H and SO_2NH_2, exchange with D_2O), 8.03 (1H, s, Ar−H), 9.09 (1H, s, Ar−NH, exchange with D_2O); δ_C (100 MHz, DMSO-d_6) 38.3, 53.0, 54.8, 115.6, 119.5, 121.5, 127.8, 129.4, 130.2, 130.4, 137.9, 141.5, 145.7, 155.5, 173.5; ESI-HRMS (m/z) calculated for $[M + H]^+$ ion species $C_{17}H_{20}N_3O_5S$ 378.1118, found 378.1117.

*Synthesis of (±)-Dimethyl((3-sulfamoylphenyl)carbamoyl)-aspartate (**12d**).* (±)-Dimethyl((3-sulfamoylphenyl)carbamoyl)-aspartate **12d** was obtained according to the general procedure previously reported using 3-aminobenzenesulfonamide **1b** and (±)-aspartic acid dimethylester hydrochloride **6d**. The crude compound was obtained after trituration from ethyl ether followed by silica gel column chromatography. Yield 71%; m.p. 64−65 °C; silica gel TLC R_f 0.50 (MeOH/DCM 10% v/v); δ_H (400 MHz, DMSO-d_6) 2.92 (2H, m, $-CH_2$), 3.67 (3H, s, $-OCH_3$), 3.70 (3H, s, $-OCH_3$), 4.70 (1H, m, −NHCH), 6.79 (1H, d, J = 8.0 Hz, CONHCH, exchange with D_2O), 7.35 (2H, s, SO_2NH_2, exchange with D_2O), 7.40−7.52 (3H, m, Ar−H), 8.04 (1H, s, Ar−H), 9.19 (1H, s, Ar−NH, exchange with D_2O); δ_C (100 MHz, DMSO-d_6) 37.3, 50.0, 52.8, 53.4, 115.7, 119.6, 121.6, 130.4, 141.5, 145.7, 155.5, 172.0, 172.8; ESI-HRMS (m/z) calculated for $[M + H]^+$ ion species $C_{13}H_{18}N_3O_7S$ 360.0860, found 360.0863.

*Synthesis of (±)-Methyl((3-sulfamoylphenyl)carbamoyl)-methioninate (**12e**).* (±)-Methyl ((3-sulfamoylphenyl)carbamoyl)-methioninate **12e** was obtained according to the general procedure previously reported using 3-aminobenzenesulfonamide **1b** and (±)-methionine methylester hydrochloride **6e**. The crude compound was obtained after trituration from petroleum ether followed by silica gel column chromatography. Yield 47%; m.p. 86−87 °C; silica gel TLC R_f 0.52 (MeOH/DCM 10% v/v); δ_H (400 MHz, DMSO-d_6) 2.00 (2H, m, $-CH_2S-$), 2.01 (3H, s, $-SCH_3$), 3.36 (2H, m, $-CH_2$), 3.71 (3H, s, $-OCH_3$), 4.41 (1H, m, −CH), 6.82 (1H, d, J = 7.6 Hz, CONH, exchange with D_2O), 7.34 (2H, s, SO_2NH_2, exchange with D_2O), 7.39−7.51 (3H, m, Ar−H), 8.05 (1H, s, −CONHCH), 9.03 (1H, s, Ar−NH, exchange with D_2O); δ_C (100 MHz, DMSO-d_6) 15.7, 30.5, 32.1, 52.5, 53.1, 115.7, 119.5, 121.7, 130.4, 141.5, 145.7, 155.7, 174.0; ESI-HRMS (m/z) calculated for $[M + H]^+$ ion species $C_{13}H_{20}N_3O_5S_2$ 362.0839, found 362.0836.

In Vitro Carbonic Anhydrase Inhibition Assay. The CA-catalyzed CO_2 hydration activity was performed using an Applied Photophysics stopped-flow instrument using phenol red, at a concentration of 0.2 mM, as a pH indicator with 20 mM HEPES (pH 7.5) as the buffer, 20 mM Na_2SO_4, and following the initial rates of the CA-catalyzed CO_2 hydration reaction for a period of 10−100 s and working at the maximum absorbance of 557 nm.[23] The CO_2 concentrations ranged from 1.7 to 17 mM. For each inhibitor, six traces of the initial 5−10% of the reaction mixture have been used in order to determine the initial velocity. The uncatalyzed reaction rates were determined in the same manner and subtracted from the total observed rates. Stock solutions of inhibitor (0.1 mM) were prepared in distilled water, and dilutions up to 0.01 nM were prepared. Solutions containing the inhibitor and the enzyme were preincubated for 15 min at room temperature prior to the assay in order to allow the formation of the E−I complex. The inhibition constants were obtained as nonlinear least-squares protocols using PRISM 3[25−27] and are the mean from at least three different measurements. All hCAs were recombinant ones and were obtained in house.[25−29]

Crystallization and X-ray Data Collection. The crystals of hCA II in complex with **10g** were obtained using the hanging drop vapor diffusion method using a 24-well Linbro plate. Two microliters of 10 mg/mL solution of hCA II in Tris−HCl, 20 mM, pH 8.0 was mixed with 2 μL of a solution of 1.5 M sodium citrate and 0.1 M Tris, pH 8.0 and was equilibrated against the same solution at 296 K. Crystals of the protein grew in 1 week. Afterward, the hCA II crystals were soaked in a 5 mM inhibitor solution for 3 days. The crystals were flash-frozen at 100 K using a solution obtained by adding 15% (v/v) glycerol to the mother liquor solution as a cryoprotectant. Data on the crystal of the complex with **10g** were collected using synchrotron radiation at the ID-11.2C beamline at Elettra (Trieste, Italy) with a wavelength of 1.000 Å and a Pilatus3 6M Dectris CCD detector.

Inhibitors **7c** and **11f** were cocrystallized with hCA II via the hanging drop vapor diffusion method. A volume of 0.5 mL of mother liquor (1.6 M sodium citrate and 50 mM Tris at pH 7.8) was used in each well to set up crystal trays. Each crystallization drop contained a 1:1 ratio of 10 mg/mL protein to mother liquor. The inhibitors were dissolved in 100% DMSO and further diluted to ∼100 μM DMSO in the crystallization drop. Crystals of hCA II were observed within 1 week. Diffraction data on crystals of the complexes of hCA II with **7c** and **11f** were collected on the F1 beamline at the Cornell High Energy Synchrotron Source (CHESS) and at the Stanford Synchrotron Radiation Lightsource (SSRL) at a 0.977 Å wavelength. A Pilatus 6M detector was utilized to collect the data sets with a crystal-to-detector distance of 240 mm, 1 degree oscillation, and 1 s image exposure, and a total of 360 images was collected at CHESS. An Eiger detector was utilized at SSRL to collect the data set with a crystal-to-detector distance at 120 mm, 0.15 degree oscillation, and 1 s image exposure, for a total of 1200 images. The diffraction data were indexed and integrated with XDS.[30] Data were scaled in the space group $P21$ via AIMLESS[31] in the CCP4 program suite.[32]

Structure Determination and Refinement. The crystal structure of hCA II (PDB accession code: 3P58) without solvent molecules and other heteroatoms was used to obtain the initial phases of the structure of the complex of hCA II with **11g** using Refmac5.[33] Unique reflections (5%) were selected randomly and excluded from the refinement data set for the purpose of Rfree calculations. The initial $|F_o - F_c|$ difference electron density maps unambiguously showed the inhibitor molecules. Atomic models for inhibitors were calculated and energy-minimized using the program JLigand 1.0.40.[34] Refinements were proceeded using normal protocols of positional, isotropic atomic displacement parameters alternating with manual building of the models using COOT.[35] Solvent molecules were introduced automatically using the program ARP.[36] The quality of the final models was assessed with COOT and RAMPAGE.[37] Atomic coordinates were deposited in the Protein Data Bank (PDB accession code: 7ASJ). Graphical representations were generated with Chimera.[38] For the complexes of hCA II with **7c** and **11f**, molecular replacement was used to determine the phases with PDB: 3KS3[39] as the search model. Model modifications were performed in COOT[40] such as adding in inhibitor, zinc, water, and ligand (glycerol) to the active site along with ligand PDB file modifications. Phenix[41] generated ligand restraint files and performed refinements. PyMol (Schrödinger) generated figures.

Protein Expression and Purification. Competent BL21 *Escherichia coli cells* were transformed with plasmid DNA with the hCA II gene insert using standard protocols.[42,43] The cell culture was grown overnight in LB followed by large-scale growth the next day until OD_{600} reached ∼0.6. At this point, 0.5 mM isopropyl β-D-1-thiogalactoside and 1 mM zinc sulfate were added to induce protein expression for 3 h. The culture was pelleted and frozen overnight to be lysed later via a microfluidizer at 18,000 PSI. Following centrifugation of the lysate, the supernatant was filtered with 0.4 μm filters before running over an affinity column containing *p*-aminomethyl-benzenesulfonamide agarose. hCA II was eluted with azide and then buffer-exchanged into a storage buffer (50 mM Tris pH 7.8) to remove azide from the active site. The protein purity was determined with a 12% SDS-PAGE, and the protein concentration was measured with UV/vis spectroscopy at 280 nm.

Hypertensive Rabbit IOP-Lowering Studies. Adult male New Zealand albino rabbits weighing 2−2.5 kg were employed in this study. The animals were divided into groups of four for each of the chosen specific treatments. All experiments were performed in accordance with the European Community Guidelines for the Care and Use of

https://doi.org/10.1021/acs.jmedchem.1c01906
J. Med. Chem. 2022, 65, 824−837

Laboratory Animals (2010/63/EU) and the Italian Legislative Decree 26 (13/03/2014) and approved by the Animal Care Committee of the University of Florence and Italian Ministry of Health (authorization n. 318/2018-PR). Experiments involving animals were reported according to Animal Research: Reporting of in Vivo Experiments (ARRIVE) guidelines.[44] Every effort was made to minimize animal suffering and to reduce the number of animals used. The rabbits were kept in individual cages; food and water were provided ad libitum. The animals were identified with a tattoo on the ear, numbered consecutively, and maintained on a 12 h−12 h light/dark cycle in a temperature-controlled room (22−23 °C). All selected animals were examined before the beginning of the study and were determined to be normal on ophthalmic and general examinations. All the compounds were dissolved in pyrogen-free sterile 0.9% NaCl solution at 1% concentration plus 1% DMSO and 0.1% EtOH. The viability of the tested compounds was evaluated after fire repeated administration on consecutive days using the Draize eye test.[45]

Glaucoma was induced by injection of 0.1 mL of 0.25% carbomer (Siccafluid, FarMila−THEA Pharmaceuticals) into the anterior eye chamber bilaterally in New Zealand albino rabbits anesthetized with a mixture of ketamine and xylazine (35 and 5 mg/kg, body weight, i.m.) using the procedure previously reported.[46] IOP was measured before carbomer injection (basal) and three times a day until stabilization. All rabbits treated with carbomer presented a net increase in IOP. One drop of 0.2% oxybuprocaine hydrochloride (Novesine, Sandoz) diluted 1:1 with sterile saline was instilled in each eye immediately before each set of pressure measurements. IOP was measured using a pneumotonometer Reichert, model 30 (Reichert, Inc., Depew, NY) as reported earlier.[46] The pressure readings were matched with two-point standard pressure measurements at 1, 2, and 4 h after the instillation of the drug and once a day for the subsequent days using a Digilab calibration verifier. All IOP measurements were conducted by the same investigators using the same tonometer. As soon as a stable IOP increase was obtained, the animals were treated with the drugs in study. The efficacy of the different drugs in lowering IOP was evaluated after drug administration over 4 h, with the following schedule: before and after 30, 60, 120, and 240 min after drug administration. The treatment was performed in four animals per drug in one eye and compared to the contralateral eye treated with vehicle (0.9% NaCl, 0.1% DMSO, and 0.1% EtOH). A group of four nonglaucomatous albino rabbits was treated with the drugs of this study and used as a control. At the end of the experiments, the animals were killed with a lethal dose of pentothal (0.5 mL/kg, body weight, e.v., Abbott SpA, Campoverde di Aprilia, IT).

■ ASSOCIATED CONTENT

Supporting Information

The Supporting Information is available free of charge at https://pubs.acs.org/doi/10.1021/acs.jmedchem.1c01906.

SMILES representation for compounds (CSV)

Reaction conditions explored (Table S1), HPLC traces of final compounds, and summary of data collection and atomic model refinement statistics (Tables S2−S4). Authors will release the atomic coordinates upon article publication (PDF)

■ AUTHOR INFORMATION

Corresponding Authors

Fabrizio Carta − *NEUROFARBA Department, Sezione di Scienze Farmaceutiche e Nutraceutiche, University of Florence, 50019 Florence, Italy;* orcid.org/0000-0002-1141-6146; Email: fabrizio.carta@unifi.it

Claudiu T. Supuran − *NEUROFARBA Department, Sezione di Scienze Farmaceutiche e Nutraceutiche, University of Florence, 50019 Florence, Italy;* orcid.org/0000-0003-4262-0323; Email: claudiu.supuran@unifi.it

Authors

Gioele Vannozzi − *NEUROFARBA Department, Sezione di Scienze Farmaceutiche e Nutraceutiche, University of Florence, 50019 Florence, Italy*

Daniela Vullo − *NEUROFARBA Department, Sezione di Scienze Farmaceutiche e Nutraceutiche, University of Florence, 50019 Florence, Italy*

Andrea Angeli − *NEUROFARBA Department, Sezione di Scienze Farmaceutiche e Nutraceutiche, University of Florence, 50019 Florence, Italy;* orcid.org/0000-0002-1470-7192

Marta Ferraroni − *Dipartimento di Chimica " Ugo Schiff", University of Florence, 50019 Florence, Italy;* orcid.org/0000-0001-7258-738X

Jacob Combs − *Department of Biochemistry and Molecular Biology, College of Medicine, University of Florida, Gainesville, Florida 32610, United States*

Carrie Lomelino − *Department of Biochemistry and Molecular Biology, College of Medicine, University of Florida, Gainesville, Florida 32610, United States*

Jacob Andring − *Department of Biochemistry and Molecular Biology, College of Medicine, University of Florida, Gainesville, Florida 32610, United States;* orcid.org/0000-0002-6632-6391

Robert Mckenna − *Department of Biochemistry and Molecular Biology, College of Medicine, University of Florida, Gainesville, Florida 32610, United States*

Gianluca Bartolucci − *NEUROFARBA Department, Sezione di Scienze Farmaceutiche e Nutraceutiche, University of Florence, 50019 Florence, Italy;* orcid.org/0000-0002-5631-8769

Marco Pallecchi − *NEUROFARBA Department, Sezione di Scienze Farmaceutiche e Nutraceutiche, University of Florence, 50019 Florence, Italy*

Laura Lucarini − *NEUROFARBA Department, Section of Pharmacology and Toxicology, University of Florence, 50139 Florence, Italy*

Silvia Sgambellone − *NEUROFARBA Department, Section of Pharmacology and Toxicology, University of Florence, 50139 Florence, Italy*

Emanuela Masini − *NEUROFARBA Department, Section of Pharmacology and Toxicology, University of Florence, 50139 Florence, Italy*

Complete contact information is available at: https://pubs.acs.org/10.1021/acs.jmedchem.1c01906

Author Contributions

The manuscript was written through contributions of all authors. All authors have given approval to the final version of the manuscript.

Notes

The authors declare no competing financial interest.

■ ACKNOWLEDGMENTS

F.C. is grateful to "Bando di Ateneo per il Finanziamento di Progetti Competitivi per Ricercatori a Tempo Determinato (RTD) dell'Università di Firenze - 2020-2021," which partially funded this work.

■ DEDICATION

This paper is dedicated to the memory of Mavis Agbandje-McKenna who sadly passed away on Wednesday 3rd March, 2021.

■ ABBREVIATIONS

CA, carbonic anhydrase; AAZ, acetazolamide; DRZ, dorzolamide; CAIs, carbonic anhydrase inhibitors; IOP, intraocular pressure

■ REFERENCES

(1) Ghosh, A. K.; Brindisi, M. Urea derivatives in modern drug discovery and medicinal chemistry. *J. Med. Chem.* **2020**, *63*, 2751−2788.

(2) Ghosh, A. K.; Gemma, S. *Structure-based design of drugs and other bioactive molecules: tools and strategies*; Wiley-VCH: Weinheim, Germany, 2014.

(3) Steverding, D. The development of drugs for treatment of sleeping sickness: a historical review. *Parasit. Vectors* **2010**, *3*, 15.

(4) Nowick, J. S.; Mahrus, S.; Smith, E. M.; Ziller, J. W. Triurea Derivatives of Diethylenetriamine as Potential Templates for the Formation of Artificial β-Sheets. *J. Am. Chem. Soc.* **1996**, *118*, 1066−1072.

(5) Holmes, D. L.; Smith, E. M.; Nowick, J. S. Solid-Phase Synthesis of Artificial β-Sheets. *J. Am. Chem. Soc.* **1997**, *119*, 7665−7669.

(6) Claudon, P.; Violette, A.; Lamour, K.; Decossas, M.; Fournel, S.; Heurtault, B.; Godet, J.; Mély, Y.; Jamart-Grégoire, B.; Averlant-Petit, M. C.; Briand, J. P.; Duportail, G.; Monteil, H.; Guichard, G. Consequences of isostructural main-chain modifications for the design of antimicrobial foldamers: helical mimics of host-defense peptides based on a heterogeneous amide/urea backbone. *Angew. Chem., Int. Ed.* **2010**, *49*, 333−336.

(7) Chen, Y. Y.; Chang, L. T.; Chen, H. W.; Yang, C. Y.; Hsin, L. W. Fast and facile synthesis of 4-nitrophenyl 2-azidoethylcarbamate derivatives from N-Fmoc-protected alpha-amino acids as activated building blocks for urea moiety-containing compound library. *ACS Comb. Sci.* **2017**, *19*, 131−136.

(8) Burgess, K.; Shin, H.; Linthicum, D. S. Solid-phase syntheses of unnatural biopolymers containing repeating urea units. *Angew. Chem., Int. Ed. Engl.* **1995**, *34*, 907−909.

(9) Delebecq, E.; Pascault, J.-P.; Boutevin, B.; Ganachaud, F. On the versatility of urethane/urea bonds: reversibility, blocked isocyanate, and non-isocyanate polyurethane. *Chem. Rev.* **2013**, *113*, 80−118.

(10) Kirillova, A.; Yeazel, T. R.; Asheghali, D.; Petersen, S. R.; Dort, S.; Gall, K.; Becker, M. L. Fabrication of biomedical scaffolds using biodegradable polymers. *Chem. Rev.* **2021**, *121*, 11238−11304.

(11) Pacchiano, F.; Carta, F.; Vullo, D.; Scozzafava, A.; Supuran, C. T. Inhibition of β-carbonic anhydrases with ureido-substituted benzenesulfonamides. *Bioorg. Med. Chem. Lett.* **2011**, *21*, 102−105.

(12) Pacchiano, F.; Carta, F.; McDonald, P. C.; Lou, Y.; Vullo, D.; Scozzafava, A.; Dedhar, S.; Supuran, C. T. Ureido-substituted benzenesulfonamides potently inhibit carbonic anhydrase IX and show antimetastatic activity in a model of breast cancer metastasis. *J. Med. Chem.* **2011**, *6*, 1896−1902.

(13) Ali, M.; Angeli, A.; Bozdag, M.; Carta, F.; Capasso, C.; Farooq, U.; Supuran, C. T. Benzylaminoethylureido-tailed benzenesulfonamides show potent inhibitory activity against bacterial carbonic anhydrases. *Chem. Med. Chem.* **2020**, *15*, 2444−2447.

(14) Poli, G.; Bozdag, M.; Berrino, E.; Angeli, A.; Tuccinardi, T.; Carta, F.; Supuran, C. T. *N*-aryl-*N*′-ureido-*O*-sulfamates as potent and selective inhibitors of hCA VB over hCA VA: Deciphering the binding mode of new potential agents in mitochondrial dysfunctions. *Bioorg. Chem.* **2020**, *100*, 103896.

(15) Ali, M.; Bozdag, M.; Farooq, U.; Angeli, A.; Carta, F.; Berto, P.; Zanotti, G.; Supuran, C. T. Benzylaminoethyureido-tailed benzenesulfonamides: design, synthesis, kinetic and X-ray investigations on human carbonic anhydrases. *Int. J. Mol. Sci.* **2020**, *21*, 2560.

(16) Bozdag, M.; Ferraroni, M.; Ward, C.; Carta, F.; Bua, S.; Angeli, A.; Langdon, S. P.; Kunkler, I. H.; al-Tamimi, A. M. S.; Supuran, C. T. Carbonic anhydrase inhibitors based on sorafenib scaffold: design, synthesis, crystallographic investigation and effects on primary breast cancer cells. *Eur. J. Med. Chem.* **2019**, *182*, 111600.

(17) Bozdag, M.; Poli, G.; Angeli, A.; Lucarini, E.; Tuccinardi, T.; Di Cesare Mannelli, L.; Selleri, S.; Ghelardini, C.; Winum, J.-Y.; Carta, F.; Supuran, C. T. N-aryl-N′-ureido-O-sulfamates: potent and selective inhibitors of the human carbonic anhydrase VII isoform with neuropathic pain relieving properties. *Bioorg. Chem.* **2019**, *89*, 103033.

(18) Gallou, I. Unsymmetrical ureas. Synthetic methodologies and application in drug design. *Org. Prep. Proced. Int.* **2007**, *39*, 355−383.

(19) Lolak, N.; Akocak, S.; Bua, S.; Supuran, C. T. Design, synthesis and biological evaluation of novel ureido benzenesulfonamides incorporating 1,3,5-triazine moieties as potent carbonic anhydrase IX inhibitors. *Bioorg. Chem.* **2019**, *82*, 117−122.

(20) Brotherton, T. K.; Lynn, J. W.; Smith, J. Isocyanatophenylsulfonyl isocyanates. US3454606A1

(21) Zimmerman, C.; Babich, J. W.; Joyal, J.; Maresca, K. P.; Barone, C. Inhibitors of carbonic anhydrase IX. US2009/0175794A1

(22) Fairhurst, R. A.; Taylor, R. J.; Purine derivatives acting as A2A receptor agonists. WO2006074925A1

(23) Khalifah, R. G. The carbon dioxide hydration activity of carbonic anhydrase. I. Stop flow kinetic studies on the native human isoenzymes B and C. *J. Biol. Chem.* **1971**, *246*, 2561.

(24) Alterio, V.; di Fiore, A.; D'Ambrosio, K.; Supuran, C. T.; de Simone, G. Multiple binding modes of inhibitors to carbonic anhydrases: how to design specific drugs targeting 15 different isoforms? *Chem. Rev.* **2012**, *112*, 4421−4468.

(25) Carta, F.; Vullo, D.; Osman, S. M.; AlOthman, Z.; Supuran, C. T. Synthesis and carbonic anhydrase inhibition of a series of SLC-0111 analogs. *Bioorg. Med. Chem.* **2017**, *25*, 2569−2576.

(26) Ratto, F.; Witort, E.; Tatini, F.; Centi, S.; Lazzeri, L.; Carta, F.; Lulli, M.; Vullo, D.; Fusi, F.; Supuran, C. T.; Scozzafava, A.; Capaccioli, S.; Pini, R. Plasmonic particles that hit hypoxic cells. *Adv. Funct. Mater.* **2015**, *25*, 316−323.

(27) Vullo, D.; Durante, M.; Di Leva, F. S.; Cosconati, S.; Masini, E.; Scozzafava, A.; Novellino, E.; Supuran, C. T.; Carta, F. Monothiocarbamates strongly inhibit carbonic anhydrases in vitro and possess intraocular pressure lowering activity in an animal model of glaucoma. *J. Med. Chem.* **2016**, *59*, 5857−5867.

(28) Celik, F.; Arslan, M.; Yavuz, E.; Demir, D.; Gençer, N. Synthesis and carbonic anhydrase inhibitory properties of novel 1,4-dihydropyrimidinone substituted diarylureas. *J. Enzyme Inhib. Med. Chem.* **2014**, *29*, 18−22.

(29) Berber, N.; Arslan, M.; Yavuz, E.; Bilen, C.; Gencer, N. Synthesis and evaluation of new phthalazine urea and thiourea derivatives as carbonic anhydrase inhibitors. *J. Chem.* **2013**, 1−8.

(30) Kabsch, W. Integration, scaling, space-group assignment and post-refinement. *Acta Crystallogr. D Biol. Crystallogr.* **2010**, *66*, 133−144.

(31) Evans, P. R.; Murshudov, G. N. How good are my data and what is the resolution? *Acta Crystallogr. D Biol. Crystallogr.* **2013**, *69*, 1204−1214.

(32) Winn, M. D.; Ballard, C. C.; Cowtan, K. D.; Dodson, E. J.; Emsley, P.; Evans, P. R.; Keegan, R. M.; Krissinel, E. B.; Leslie, A. G. W.; McCoy, A.; McNicholas, S. J.; Murshudov, S. G.; Pannu, N. S.; Potterton, E. A.; Powell, H. R.; Read, R. J.; Vagin, A.; Wilson, K. S. Overview of the CCP4 suite and current developments. *Acta Crystallogr. D Biol. Crystallogr.* **2011**, *67*, 235−242.

(33) Murshudov, G. N.; Vagin, A. A.; Dodson, E. J. Refinement of macromolecular structures by the maximum-likelihood method. *Acta Crystallogr., Sect. D: Biol. Crystallogr.* **1997**, *53*, 240−255.

(34) Lebedev, A. A.; Young, P.; Isupov, M. N.; Moroz, O. V.; Vagin, A. A.; Murshudov, G. N. JLigand: a graphical tool for the CCP4 template restraint library. *Acta Crystallogr., Sect. D: Biol. Crystallogr.* **2012**, *68*, 431−440.

(35) Emsley, P.; Lohkamp, B.; Scott, W. G.; Cowtan, K. Features and development of Coot. *Acta Crystallogr., Sect. D: Biol. Crystallogr.* **2010**, *66*, 486−501.

(36) Lamzin, V. S.; Perrakis, A.; Wilson, K. S. The ARP/wARP suite for automated construction and refinement of protein models. In *International Tables for Crystallography*, 1st ed.; Rossmann, M. G., Arnold, E., Eds.; Kluwer Academic: Dordrecht, 2001; p. 311.

https://doi.org/10.1021/acs.jmedchem.1c01906
J. Med. Chem. 2022, 65, 824−837

(37) Lovell, S. C.; Davis, I. W.; Arendall, W. B., III; de Bakker, P. I. W.; Word, J. M.; Prisant, M. G.; Richardson, J. S.; Richardson, D. C. Structure validation by Cα geometry: ϕ, ψ and Cβ deviation. *Proteins* **2003**, *50*, 437−450.
(38) Pettersen, E. F.; Goddard, T. D.; Huang, C. C.; Couch, G. S.; Greenblatt, D. M.; Meng, E. C.; Ferrin, T. E. UCSF Chimera-A visualization system for exploratory research and analysis. *J. Comput. Chem.* **2004**, *25*, 1605−1612.
(39) Avvaru, B. S.; Kim, C. U.; Sippel, K. H.; Gruner, S. M.; Agbandje-McKenna, M.; Silverman, D. M.; McKenna, R. A short, strong hydrogen bond in the active site of human carbonic anhydrase II. *Biochemistry* **2010**, *49*, 249−251.
(40) Emsley, P.; Cowtan, K. Coot: model-building tools for molecular graphics. *Acta Crystallogr. D Biol. Crystallogr.* **2004**, *60*, 2126−2132.
(41) Adams, P. D.; Afonine, P. V.; Bunkóczi, G.; Chen, V. B.; Davis, I. W.; Echols, N.; Headd, J. J.; Hung, L.-W.; Kapral, G. J.; Grosse-Kunstleve, R. W.; McCoy, A. J.; Moriarty, N. W.; Oeffner, R.; Read, R. J.; Richardson, D. C.; Richardson, J. S.; Terwilliger, T. C.; Zwart, P. H. PHENIX: a comprehensive Python-based system for macromolecular structure solution. *Acta Crystallogr. D Biol. Crystallogr.* **2010**, *66*, 213−221.
(42) Pinard, M. A.; Boone, C. D.; Rife, B. D.; Supuran, C. T.; McKenna, R. Structural study of interaction between brinzolamide and dorzolamide inhibition of human carbonic anhydrases. *Bioorg. Med. Chem.* **2013**, *21*, 7210−7215.
(43) Tanhauser, S. M.; Jewell, D. A.; Tu, C. K.; Silverman, D. N.; Laipis, P. J. A T7 expression vector optimized for site-directed mutagenesis using oligodeoxyribonucleotide cassettes. *Gene* **1992**, *117*, 113−117.
(44) Kilkenny, C.; Browne, W.; Cuthill, I. C.; Emerson, M.; Altman, D. G.; NC3Rs reporting guidelines working group. Animal research: reporting in vivo experiments: the ARRIVE guidelines. *Br. J. Pharmacol.* **2010**, *160*, 1577−1579.
(45) Wilhelmus, K. R. The Draize eye test. *Surv. Ophthalmol.* **2001**, *45*, 493−515.
(46) Lanzi, C.; Lucarini, L.; Durante, M.; Sgambellone, S.; Pini, A.; Catarinicchia, S.; Łażewska, D.; Kieć-Kononowicz, K.; Stark, H.; Masini, E. Role of histamine H 3- receptor antagonists on intraocular pressure reduction in rabbit models of transient ocular hypertension and glaucoma. *Int. J. Mol. Sci.* **2019**, *20*, 981−986.

Recommended by ACS

Rapid Total Synthesis of Iheyamine A via a Pictet–Spengler/Redox-Mediated Cyclization Cascade
Ya Wu, Sheng Liu, *et al.*
MARCH 23, 2023
THE JOURNAL OF ORGANIC CHEMISTRY
READ

Exploring SPK98 for the Selective Sensitization of ATM- or P53-Deficient Cancer Cells
Bhanu Priya, Sivapriya Kirubakaran, *et al.*
JANUARY 30, 2023
ACS OMEGA
READ

Transporter Inhibition Profile for the Antivirals Tilorone, Quinacrine and Pyronaridine
Patricia A. Vignaux, Sean Ekins, *et al.*
MARCH 24, 2023
ACS OMEGA
READ

Design, Synthesis, and Biological Evaluation Studies of Novel Naphthalene-Chalcone Hybrids As Antimicrobial, Anticandidal, Anticancer, and VEGFR-2 Inhibitors
Derya Osmaniye, Zafer Asım Kaplancıklı, *et al.*
FEBRUARY 13, 2023
ACS OMEGA
READ

Get More Suggestions >

https://doi.org/10.1021/acs.jmedchem.1c01906
J. Med. Chem. 2022, 65, 824−837